UPPSALA
UNIVERSITET

Digital Comprehensive Summaries of Uppsala Dissertations from the Faculty of Science and Technology 1522

Finite Difference and Discontinuous Galerkin Methods for Wave Equations

SIYANG WANG

ACTA
UNIVERSITATIS
UPSALIENSIS
UPPSALA
2017

ISSN 1651-6214
ISBN 978-91-554-9927-3
urn:nbn:se:uu:diva-320614

Dissertation presented at Uppsala University to be publicly examined in Room 2446, Polacksbacken, Lägerhyddsvägen 2, Uppsala, Tuesday, 13 June 2017 at 10:15 for the degree of Doctor of Philosophy. The examination will be conducted in English. Faculty examiner: Professor Thomas Hagstrom (Department of Mathematics, Southern Methodist University).

Abstract

Wang, S. 2017. Finite Difference and Discontinuous Galerkin Methods for Wave Equations. *Digital Comprehensive Summaries of Uppsala Dissertations from the Faculty of Science and Technology* 1522. 53 pp. Uppsala: Acta Universitatis Upsaliensis. ISBN 978-91-554-9927-3.

Wave propagation problems can be modeled by partial differential equations. In this thesis, we study wave propagation in fluids and in solids, modeled by the acoustic wave equation and the elastic wave equation, respectively. In real-world applications, waves often propagate in heterogeneous media with complex geometries, which makes it impossible to derive exact solutions to the governing equations. Alternatively, we seek approximated solutions by constructing numerical methods and implementing on modern computers. An efficient numerical method produces accurate approximations at low computational cost.

There are many choices of numerical methods for solving partial differential equations. Which method is more efficient than the others depends on the particular problem we consider. In this thesis, we study two numerical methods: the finite difference method and the discontinuous Galerkin method. The finite difference method is conceptually simple and easy to implement, but has difficulties in handling complex geometries of the computational domain. We construct high order finite difference methods for wave propagation in heterogeneous media with complex geometries. In addition, we derive error estimates to a class of finite difference operators applied to the acoustic wave equation. The discontinuous Galerkin method is flexible with complex geometries. Moreover, the discontinuous nature between elements makes the method suitable for multiphysics problems. We use an energy based discontinuous Galerkin method to solve a coupled acoustic-elastic problem.

Keywords: Wave propagation, Finite difference method, Discontinuous Galerkin method, Stability, Accuracy, Summation by parts, Normal mode analysis

Siyang Wang, Department of Information Technology, Division of Scientific Computing, Box 337, Uppsala University, SE-751 05 Uppsala, Sweden.

ISSN 1651-6214
ISBN 978-91-554-9927-3
urn:nbn:se:uu:diva-320614 (http://urn.kb.se/resolve?urn=urn:nbn:se:uu:diva-320614)

Dedicated to TDB

List of papers

This thesis is based on the following papers, which are referred to in the text by their Roman numerals.

I S. WANG, K. VIRTA AND G. KREISS, *High order finite difference methods for the wave equation with non–conforming grid interfaces*, J. Sci. Comput., 68(2016), pp 1002–1028.
Contribution: S. Wang performed the analysis, most experiments, and wrote the manuscript except Section 5.3. K. Virta wrote Section 5.3 and performed the experiments therein. The ideas were developed in close collaboration between all authors.

II S. WANG, *An improved high order finite difference method for non–conforming grid interfaces for the wave equation*, in review, available as preprint arXiv:1702.02056.
Contribution: S. Wang is the sole author of the manuscript.

III S. WANG AND G. KREISS, *Convergence of summation–by–parts finite difference methods for the wave equation*, J. Sci. Comput., 71(2017), pp. 219–245.
Contribution: S. Wang performed the analysis and experiments. The manuscript was written by S. Wang with significant input from G. Kreiss. The ideas were developed in close collaboration between both authors.

IV S. WANG, A. NISSEN AND G. KREISS, *Convergence of finite difference methods for the wave equation in two space dimensions*, in review, available as preprint arXiv:1702.01383.
Contribution: S. Wang took the lead in performing the analysis, designing the experiments, and writing the manuscript, with significant input from A. Nissen and G. Kreiss. The ideas were developed in close collaboration between all authors.

V D. APPELÖ AND S. WANG, *An energy based discontinuous Galerkin method for acoustic-elastic waves*, technical report.
Contribution: The authors derived the method together. Software implementation of the method and writing of the manuscript were carried out in a collaborative spirit with D. Appelö taking the lead.

Contents

1. Introduction

The fascinating subject of wave motion finds practical applications in a wide range of science and industry. In fact, waves are integrated in our life. Dating back to pre–modern period, long–distant communications rely on, for example, sending audio messages via loud horns, an application of acoustic wave propagation. Thanks to electromagnetic waves used in telecommunication, nowadays multimedia information can be transported instantly. Waves can also have negative effects. Seismic waves created by a sudden release of energy in the earth result in earthquakes, which cause damages to humans and society. These examples represent the motivation of studies of wave motion.

Waves can be distinguished by their characteristics. For example, based on the ability to transport energy through a vacuum, waves can be categorized into mechanical waves and electromagnetic waves. Mechanical waves can only propagate through a medium, whereas propagation of an electromagnetic wave does not require a medium. Sound and light are familiar examples of mechanical waves and electromagnetic waves, respectively. In this thesis, we study two important mechanical waves: acoustic waves in gases or fluids, and elastic waves in solids.

Mathematically, wave propagation is modeled by partial differential equations, with media properties described by coefficients in the governing equations. In an ideal environment when waves propagate in a homogeneous unbounded domain, analytical solutions to the governing equations can be derived. However, real–world applications provide inhomogeneities, discontinuities, and obstacles with complex geometries. These factors make wave propagation much more complicated, as reflections, refractions and mode conversions occur. As a consequence, solutions to the governing equations can be written by means of analytic expressions only in very special cases. For problems in more general settings, we seek accurate approximations of exact solutions by using numerical methods. The numerical methods are then implemented on modern computers to provide numerical simulations to improve our understanding of wave propagation, and to answer important questions in science and technology.

This thesis has contributions to two numerical methods: finite difference methods and discontinuous Galerkin methods. Finite difference methods are efficient in solving wave propagation problems on rectangular–shaped domains with Cartesian grids, but have difficulties in handling complex geometries and material discontinuities. To overcome these difficulties, we have developed a finite difference method for acoustic wave propagation in inhomogeneous media with complex geometries. The computational domain is

divided into subdomains at material discontinuities, and the subdomains are coupled numerically by interpolation. Geometric features at boundaries and interfaces are captured by using curvilinear grids, which are constructed independently in each subdomain according to material properties. The method is energy–stable and high–order accurate.

When using a finite difference method to solve an initial–boundary–value problem, for stability the truncation error is usually larger at boundaries than in the interior. A natural question is then how the boundary truncation error affects the overall accuracy of the numerical solution. To determine the rate of convergence, we have performed a normal mode analysis for a class of finite difference methods applied to the acoustic wave equation in one and two space dimensions.

Discontinuous Galerkin methods can be energy–stable and arbitrarily high–order accurate. In addition, complex geometries can be represented accurately by using unstructured grids. We have applied an energy–based discontinuous Galerkin method to study wave propagation in fluid–solid coupled media.

In the following section, we introduce concepts of acoustic and elastic wave propagation, including physical properties, governing equations, boundary and interface interactions. We also give an introduction of numerical techniques for solving the governing equations. We then specialize to two numerical methods that are central to this thesis: the finite difference method in Chapter 3 and the discontinuous Galerkin method in Chapter 4. Many interesting scientific problems can be seen as a continuation of this thesis work, and some of them are mentioned in Chapter 5.

2. Acoustic and elastic waves

2.1 Acoustic waves

The wave equation in one space dimension

$$\frac{1}{c^2} p_{tt} = p_{xx} \tag{2.1}$$

was discovered by d'Alembert in 1746 by a study of string vibrations. The scalar partial differential equation (PDE) (2.1) concerns a time variable t and a space variable x. The unknown variable $p(x,t)$ measures the displacement of the vibrating string. The string in consideration here has an infinite length $x \in (-\infty, \infty)$, thus reflections from boundaries are not involved. Later, d'Alembert suggested that sound propagation in air is also governed by (2.1), where $p(x,t)$ models the pressure disturbance of the acoustic wave with a constant wave speed $c > 0$.

2.1.1 Wave propagation

The wave equation (2.1) has second derivatives in time and space. Therefore, two initial conditions $p(x,0) = p_0(x)$ and $p_t(x,0) = p_1(x)$ should be provided in the model. The equation is sometimes called the second–order wave equation to distinguish from the advection equation with first–order derivatives in time and space.

One year after the discovery of the wave equation (2.1) , d'Alembert derived a general solution known as the d'Alembert solution

$$p = f(x - ct) + g(x + ct). \tag{2.2}$$

The wave is described by two arbitrary wave functions f and g, which are determined by the initial conditions and any forcing in the system.

An observation from the d'Alembert solution (2.2) is that at any time $t = t_0$ the wave function $f(x - ct_0)$ is simply $f(x)$ shifted to the right by a distance ct_0, and $g(x + ct_0)$ is $g(x)$ shifted to the left by the same distance ct_0. In other words, the solution p consists of two wave functions f and g, with the former one propagating to the right and the latter one propagating to the left with the same speed c. In addition, the shape of the two waves does not change in time, see Figure 2.1.

If a small perturbation of f occurs at position x_0, it takes time $|x_1 - x_0|/c$ for the perturbation traveling to the point x_1. Generally speaking, a perturbation

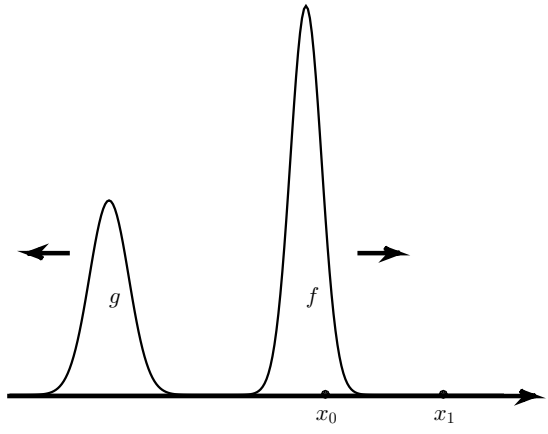

Figure 2.1. Propagation of two waves in the opposite direction

in the data travels at a finite speed in space, and not all points in space feel the perturbation immediately. This is a fundamental property of hyperbolicity, and is in contrast to parabolic and elliptic problems where all points in space feel a perturbation at once.

Characteristics

From another point of view, the solution p in (2.2) is constant on the characteristics lines $x - ct = \alpha$ and $x + ct = \beta$ with constant α, β. For a more general case with variable coefficients, characteristics lines become characteristics curves. Information carried by the PDE flows along characteristics, and the PDE is usually in a much simplified form on characteristics. The concept characteristics is important in the theory of hyperbolic partial differential equations. For example, by analyzing characteristics we can obtain proper boundary conditions that lead to a well–posed problem.

Plane waves

We specialize the d'Alembert solution (2.2) to a plane wave by considering $f(y) = A\cos(\lambda y)$ and $g = 0$ so that

$$p = A\cos(\lambda x - \omega t), \tag{2.3}$$

where $\omega = c\lambda$, see an illustration in Figure 2.2. Several quantities of interest of waves can be seen in this simple plane wave solution:

- A is the amplitude of the wave,
- λ is the wave number,
- ω is the angular frequency of the wave.

The solution p is periodic both in time and space. The temporal period of the wave is given by $T = 2\pi/\omega$, and the wave length is $l = 2\pi/\lambda$. They satisfy the

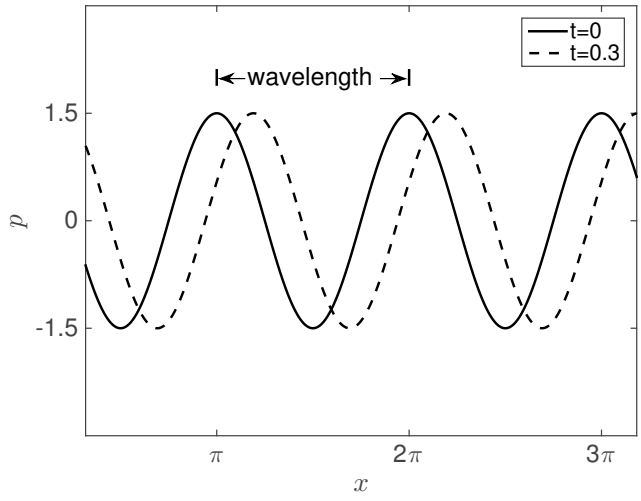

Figure 2.2. A plane wave $A\cos(\lambda x - \omega t)$ with amplitude $A = 1.5$ and wave number $\lambda = 2$. The wave moves to the right in time.

fundamental relation $c = l/T$. As we shall see in Section 2.3, wave length is an important concept for efficient numerical simulations of wave propagation.

Since the wave equation is linear, by the superposition principle, two plane waves $f(x-ct) = A\cos(\lambda x - \omega t)$ and $g(x+ct) = A\cos(\lambda x + \omega t)$ with the same wave speed, angular frequency and amplitude but traveling in the opposite directions result in a standing wave solution

$$p = 2A\cos(\lambda x)\cos(\omega t).$$

2.1.2 The acoustic wave equation

Euler derived the same equation (2.1) from the fluid dynamics perspective in 1759, and shortly afterwards extended the equation to three space dimensions. Due to the consideration of acoustics in the derivation, the wave equation is often called the acoustic wave equation, though the same equation can also model other types of wave propagation, for example, in electromagnetic and elasticity. The equation can be written in a second–order pressure form, or a first–order pressure–velocity form.

Second–order pressure form

The acoustic wave equation in terms of the acoustic pressure $p(\mathbf{x},t)$ can be written

$$\frac{1}{c^2}p_{tt} = \rho\nabla\cdot\left(\frac{1}{\rho}\nabla p\right), \tag{2.4}$$

where $\mathbf{x} \in \Re^d$ denotes the coordinates in d space dimensions, $\rho(\mathbf{x})$ is the density of the medium, and $c(\mathbf{x})$ is the wave speed. A function modeling an exter-

nal force can be added to the right–hand side of (2.4). The density and wave speed are related through the bulk modulus B as $c^2 = B/\rho$. Bulk modulus is a property of the medium, measuring how much the material compresses under an external pressure. When density gradient is neglected, the first term on the right–hand side of (2.4) simplifies to the Laplacian of p.

The acoustic wave equation (2.4) models wave propagation in a fluid (gas and liquid) with a few assumptions on the medium such as that the fluid is inviscid with negligible heat conduction and gravity effect, and is in a thermodynamic equilibrium [111]. To derive the acoustic wave equation, we regard an acoustic disturbance as a perturbation of small amplitude to an ambient state of an inviscid flow, which is characterized by the pressure, density and fluid velocity when the perturbation is absent. By using the Euler's equations of conservation of mass, momentum and energy, the wave equation is obtained after a linearization, known as the acoustic approximation, of the nonlinear equations [95].

A fluid is irrotational if the curl of the fluid velocity is zero $\nabla \times \mathbf{u} = 0$. If in addition the medium is simply–connected and the density is constant, the velocity field can then be described by the gradient of a scalar function ψ known as the velocity potential,

$$\mathbf{u} = \nabla \psi. \tag{2.5}$$

The velocity potential satisfies

$$\frac{1}{c^2}\psi_{tt} = \nabla \cdot (\nabla \psi), \tag{2.6}$$

which is in the same form as the wave equation. The velocity potential ψ is an abstract concept, but in certain cases it is more convenient to work with (2.6) than (2.4). When ψ is known after solving equation (2.6), the velocity field is given in (2.5). In addition, the acoustic pressure p can easily be obtained by the Bernoulli's principle as $p = -\rho \partial \psi / \partial t$.

First–order pressure–velocity form

The acoustic wave equation can also be formulated as a first–order hyperbolic system in terms of the pressure p and velocity field $\mathbf{u}$.

$$\frac{\partial p}{\partial t} = -B \nabla \cdot \mathbf{u}, \tag{2.7}$$

$$\rho \frac{\partial \mathbf{u}}{\partial t} = -\nabla p. \tag{2.8}$$

We recognize (2.8) as the linearized Euler's equation with a constant density.

2.1.3 Boundaries and interfaces

We have so far considered the acoustic wave equation in free space. In reality, waves often encounter obstacles in a bounded medium Ω, which is interpreted

mathematically as boundary conditions on $\partial\Omega$. Important examples include a Dirichlet boundary condition

$$p = 0, \quad \partial\Omega,$$

on a free surface and a Neumann boundary condition

$$\nabla p \cdot \mathbf{n} = 0, \quad \partial\Omega,$$

modeling waves impinging on a hard surface, where $\mathbf{n}$ is the outward pointing normal of $\partial\Omega$. Waves can also propagate from one medium Ω_1 to another medium Ω_2. Interface conditions on $\Omega_1 \cap \Omega_2$ are given by the physical properties of the two media.

When boundaries and interfaces are present in the model, it is important to make sure that the problem is well–posed. A well–posed problem has a unique solution and the solution depends continuously on the data. For a complete theory of well–posedness, we refer to [49, 50] for first–order hyperbolic systems and parabolic systems, and to [64] for second–order hyperbolic systems. The acoustic wave equation with Dirichlet or Neumann boundary conditions is well–posed.

In addition to boundary and interface phenomena, spatial dependences or even discontinuities of material parameters make it impossible to derive an analytical solution to the governing equation. Instead, seeking an accurate numerical approximation is a feasible and adequate alternative to understand wave propagation in a complicated setting. Difficulties lie in numerical treatments of boundary and interface conditions in a stable and accurate manner.

Traditionally, numerical methods are developed for the wave equation in the first–order formulation (2.7)–(2.8). An obvious drawback of solving (2.7)–(2.8) instead of the second–order formulation is that there are more unknown variables, thus more computational work is required. In addition, the initial and boundary data of the velocity field may not be provided in the model. Many recent developments concern numerical techniques for the wave equation in the original second–order form, which is also the formulation used in this thesis.

The first contribution of this thesis is devoted to a study of acoustic wave propagation in an inhomogeneous medium, with an emphasize on numerical interface techniques. The mathematical problem is formulated as follows.

Problem 1. *Consider the acoustic wave equation in an inhomogeneous medium Ω with discontinuous parameters. Assume the domain Ω can be partitioned into non–overlapping subdomains $\Omega_i, i = 1, \cdots, k$ with $\Omega = \cup\Omega_i$, and in each subdomain the material parameters c_i, ρ_i, and the forcing F_i are compatible, smooth functions with compact support. We seek solutions to the equations*

$$\frac{1}{c_i^2}\frac{\partial^2 p_i}{\partial t^2} = \rho_i \nabla \cdot \left(\frac{1}{\rho_i}\nabla p_i\right) + F_i, \quad \mathbf{x} \in \Omega_i,$$

with suitable initial conditions and boundary conditions. At an interface between two adjacent subdomains, the solutions satisfy the interface conditions

$$p_i(\mathbf{x},t) = p_j(\mathbf{x},t), \tag{2.9}$$

$$\frac{1}{\rho_i}\nabla p_i(\mathbf{x},t)\cdot\mathbf{n} = \frac{1}{\rho_j}\nabla p_j(\mathbf{x},t)\cdot\mathbf{n}, \tag{2.10}$$

on $\mathbf{x}\in\Omega_i\cap\Omega_j$, *where* $\mathbf{n}$ *is a normal of the interface between* Ω_i *and* Ω_j.

The first interface condition (2.9) corresponds to a balance of forces. By using equation (2.8), the second interface condition (2.10) can be interpreted as the fluid velocity in the normal direction being continuous across the interface, i.e. the two fluids are attached together without gap.

2.2 Elastic waves

Elasticity is an important branch of continuum mechanics. Consider an object with an external force acting on it. While the force leads to a deformation of the object, the internal force resists the deformation. When the external force is removed, if the shape of the object recovers back to its original form then the object is said to be elastic. Two important concepts in elasticity are strain and stress.

We in particular consider linear elasticity, which deals with elastic objects undergoing small deformations under external forces. This assumption holds for many engineering purposes when the external force is small. In this case, strain and stress have a linear relation governed by the Hooke's law. We refer to [45] for a comprehensive discussion on elastic waves.

2.2.1 Hooke's law

Consider a helical spring with one fixed end and one free end in a one dimensional setting. A force F applie to the free end is related linearly to the change in length X of the spring via the Hooke's spring law

$$F = -kX, \tag{2.11}$$

where k is the spring constant.

In a linear elastic medium in three space dimensions, the analogue of F and X in (2.11) are the stress σ and strain $\mathbf{e}$, respectively. Unlike the scalar quantities in (2.11), the stress and strain are second order tensors that are related via a fourth order stiffness tensor $\mathbf{C}$ as

$$\sigma = -\mathbf{C}\mathbf{e}. \tag{2.12}$$

Both the stress tensor σ and strain tensor $\mathbf{e}$ have $3^2 = 9$ components, and the stiffness tensor $\mathbf{C}$ has $3^4 = 81$ components. Thanks to the inherent symmetry, there are only 21 independent parameters in the stiffness tensor, describing an inhomogeneous anisotropic elastic material.

The stress tensor, strain tensor and traction

The stress tensor σ determines the stress at a point in the elastic medium at a certain time and strain tensor $\mathbf{e}$ characterizes the deformation of an elastic body. They can be written in matrix form

$$\sigma = \begin{bmatrix} \sigma_{11} & \sigma_{12} & \sigma_{13} \\ \sigma_{21} & \sigma_{22} & \sigma_{23} \\ \sigma_{31} & \sigma_{32} & \sigma_{33} \end{bmatrix}, \quad \mathbf{e} = \begin{bmatrix} e_{11} & e_{12} & e_{13} \\ e_{21} & e_{22} & e_{23} \\ e_{31} & e_{32} & e_{33} \end{bmatrix}.$$

Due to symmetry, the identity $\sigma_{ij} = \sigma_{ji}$ and $e_{ij} = e_{ji}$ hold for $i, j = 1, 2, 3$. By taking advantage of this symmetry property, we can write both σ and $\mathbf{e}$ in the Vigot notation as a six–by–one vector. Then the stiffness tensor can be expressed by a six–by–six matrix.

The traction on a surface is related to the stress tensor via the unit normal vector of the surface $\mathbf{n}$ as

$$\mathbf{T}^{(\mathbf{n})} = \sigma \cdot \mathbf{n}.$$

A free surface is modeled by a traction free boundary condition, $\mathbf{T}^{(\mathbf{n})} = \mathbf{0}$, and is often difficult to impose numerically in a stable and accurate manner.

2.2.2 The elastic wave equation

Second–order displacement form

The elastic wave equation can be derived by the fundamental conservation principles in mechanics and the strain–stress relation. In an inhomogeneous anisotropic elastic medium, the elastic wave equation reads

$$\rho \frac{\partial^2 \mathbf{u}}{\partial t^2} = \nabla \cdot \sigma + \mathbf{F}, \tag{2.13}$$

subject to initial conditions

$$\mathbf{u}(\mathbf{x}, 0) = \mathbf{u_0}(\mathbf{x}), \quad \frac{\partial \mathbf{u}(\mathbf{x}, 0)}{\partial t} = \mathbf{u_1}(\mathbf{x}).$$

Here, $\rho(\mathbf{x})$ is the density of the medium, $\mathbf{x} \in \Re^d$ denotes the spatial coordinate in d dimension, the $d \times 1$ vector–valued function $\mathbf{u}(\mathbf{x}, t)$ models the displacement, σ is the stress tensor, and $F(\mathbf{x}, t)$ models an external force. We note that (2.13) is a linear second–order hyperbolic system of partial differential equations.

The elastic wave equation can be rewritten to several different but equivalent forms. Equation (2.13) is called the second–order displacement form.

When restricting to a homogeneous isotropic medium, the stiffness tensor can be described by just two parameters μ and λ, often referred to as the Lamé parameters. In this case, the stress tensor in (2.13) in three space dimensions takes the form

$$\sigma = \begin{bmatrix} (2\mu+\lambda)u_x + \lambda(v_y+w_z) & \mu(u_y+v_x) & \mu(u_z+w_x) \\ \mu(u_y+v_x) & (2\mu+\lambda)v_y + \lambda(u_x+w_z) & \mu(w_y+v_z) \\ \mu(u_z+w_x) & \mu(w_y+v_z) & (2\mu+\lambda)w_z + \lambda(u_x+v_y) \end{bmatrix},$$

where $\mathbf{x} = [x,y,z]^T$ and $\mathbf{u} = [u,v,w]^T$. The vector equivalence of (2.13) is

$$\rho \frac{\partial^2 \mathbf{u}}{\partial t^2} = (\mu+\lambda)\nabla\nabla\cdot\mathbf{u} + \mu\nabla^2\mathbf{u} + \mathbf{F}, \tag{2.14}$$

where ∇^2 is the vector Laplacian, μ and λ are constant.

Pressure and shear waves

The divergence and curl of (2.14) are

$$\rho \frac{\partial^2}{\partial t^2}(\nabla\cdot\mathbf{u}) = (2\mu+\lambda)\nabla^2(\nabla\cdot\mathbf{u}) + \nabla\cdot\mathbf{F}, \tag{2.15}$$

$$\rho \frac{\partial^2}{\partial t^2}(\nabla\times\mathbf{u}) = \mu\nabla^2(\nabla\times\mathbf{u}) + \nabla\times\mathbf{F}. \tag{2.16}$$

We note that $\nabla\cdot\mathbf{u}$ and $\nabla\times\mathbf{u}$ satisfy the acoustic wave equation with wave speeds $\sqrt{(2\mu+\lambda)/\rho}$ and $\sqrt{\mu/\rho}$, respectively. This suggests the existence of two modes, namely the pressure wave and shear wave. The pressure wave is a longitudinal wave, and is analogue to acoustic waves in gases or fluids. The shear wave, on the other hand, is a transverse wave and has a lower speed than the pressure wave. In an unbounded elastic medium, only these two types of waves can propagate independently. However, when a pressure wave impinges on a boundary or interface, it may generate both pressure and shear waves, a phenomenon known as mode conversion.

Instead of solving the original elastic wave equation (2.14), it may seem simpler to solve the two acoustic wave equations (2.15) and (2.16). However, these two equations are often coupled via initial and boundary conditions, and it is more common to perform numerical computations with (2.14) directly.

Two common forms as a first–order hyperbolic system are the velocity–strain form and velocity–stress form. In the following, we present the two forms with the velocity field $\mathbf{v}$ defined as $\mathbf{v} = \partial\mathbf{u}/\partial t$.

Velocity–strain form

$$\rho \frac{\partial \mathbf{v}}{\partial t} = \nabla\cdot(\lambda\,\mathrm{Trace}(\mathbf{e})\mathbf{I} + 2\mu\mathbf{e}) + \mathbf{F}, \tag{2.17}$$

$$\frac{\partial \mathbf{e}}{\partial t} = \frac{1}{2}(\nabla\mathbf{v} + \nabla\mathbf{v}^T), \tag{2.18}$$

where Trace($\mathbf{e}$) is the sum of elements in the main diagonal of $\mathbf{e}$, and $\mathbf{I}$ is an identity operator.

Velocity–stress form

$$\rho \frac{\partial \mathbf{v}}{\partial t} = \nabla \cdot \sigma + \mathbf{F}, \tag{2.19}$$

$$\frac{\partial \sigma}{\partial t} = \lambda (\nabla \cdot \mathbf{v}) \mathbf{I} + \mu (\nabla \mathbf{v} + \nabla \mathbf{v}^T). \tag{2.20}$$

We note that both $\mathbf{e}$ in (2.18) and σ in (2.20) are second–order tensors. In three space dimensions, the two first–order formulations, (2.17)–(2.18) and (2.19)–(2.20), are systems of nine equations, whereas the second–order formulation (2.13) is a system of three equations. Additionally, if the displacement field is needed, three more equations must be solved.

2.2.3 Boundaries and interfaces

The elastic wave equation supports more types of wave motion than the acoustic wave equation. Different wave motion can be generated by different choices of boundary and interface conditions, and material parameters. As discussed in the preceding section, pressure and shear waves can exist in an elastic medium. In the following, we give some other examples of wave motion supported in an elastic medium.

Surface waves and interface waves

In seismology, it is observed that an earthquake starts with two initial tremors of small magnitude, then follows the third, much more damaging tremor. The first two tremors are consistent with elastic theory of pressure and shear waves, the third one is not. It suggests a new type of wave motion, namely surface waves. Rayleigh first investigated surface waves in 1885, and predicted that on a free surface, a wave can be confined to the surface and decays in magnitude exponentially away from the surface. Such kind of waves are called Rayleigh waves.

Another kind of surface waves, the Love waves, were discovered by Love in 1911. Love waves can exist when a thin elastic layer with a free surface on one side is welded to another much thicker elastic layer on the other side. Love waves are confined to the interface in both layers, and decay exponentially away from the interface in the thicker elastic layer.

An analogue of Rayleigh surface waves confined to the interface between two half–space elastic media are Stoneley waves. For a detailed discussion on surface waves and interface waves, see [45].

Acoustic–elastic interface

Wave propagation in a fluid–solid coupled region has applications in marine seismic survey. When performing numerical simulations, difficulties often lie in accurate treatments of fluid–solid interfaces.

The second contribution of this thesis is the development of numerical techniques for wave propagation in a fluid–solid coupled medium. Similar to Problem 1, here again we use a second–order formulation of the governing equations. The acoustic wave equation in the fluid is formulated in terms of velocity potential (2.6), and the elastic wave equation in the solid is in the second–order displacement form (2.13). The mathematical problem is stated as below.

Problem 2. *Consider the acoustic wave equation* (2.6) *in a fluid medium* Ω^f *and the elastic wave equation* (2.13) *in a solid medium* Ω^s*. We seek solutions to the equations*

$$\frac{1}{c^2}\psi_{tt} = \nabla\cdot(\nabla\psi) + F_f, \quad \mathbf{x}\in\Omega^f,$$
$$\rho\frac{\partial^2\mathbf{u}}{\partial t^2} = \nabla\cdot\sigma + F_s, \quad \mathbf{x}\in\Omega^s,$$

with suitable initial conditions and boundary conditions. The free–slip interface conditions are

$$\nabla\psi\cdot\mathbf{n} = \frac{\partial\mathbf{u}}{\partial t}\cdot\mathbf{n}, \tag{2.21}$$
$$\frac{\partial\psi}{\partial t}\mathbf{n} = \sigma\cdot\mathbf{n}, \tag{2.22}$$

where $\mathbf{n}$ *is a normal of the interface.*

By the definition of velocity potential (2.5), we interpret the first interface condition (2.21) as the continuity of velocity in the normal direction. This means that the fluid and solid are attached together without gap. The second interface condition (2.22) can actually be seen as two conditions. We note that the traction $\sigma\cdot\mathbf{n}$ is in the normal direction. Therefore, (2.22) implies a balance of compression force, and a zero shear force. This is consistent with the fact that the fluid is inviscid and the interface is perfect–slip.

2.3 Numerical methods

In the last century, numerous numerical methods have been developed for solving partial differential equations [103]. For time–dependent problems, rapid progress was made after 1950s when computers became available for computations. In this section, we discuss numerical methods for the acoustic and elastic wave equations.

There are essentially two phases of solving a time–dependent partial differential equation: the approximation of spatial derivatives and temporal deriva-

tives. One approach is to approximate spatial derivatives first and leave temporal derivatives continuous. For wave equations in the second–order form, we are then left to solve a system of ordinary differential equations

$$\mathscr{M}\frac{\partial^2 \mathbf{u}}{\partial t^2} = \mathscr{Q}\mathbf{u} + \mathbf{f}, \tag{2.23}$$

where the vector $\mathbf{u}$ denotes the degrees of freedom in the numerical solution, and $\mathbf{f}$ contains boundary and forcing data. The matrices $\mathscr{M}$ and $\mathscr{Q}$ are constructed from spatial discretizations. The structure of $\mathscr{M}$ has an important impact on efficiency, as we need to solve a large system of linear equations with $\mathscr{M}$ as the system matrix.

The ordinary differential equations (2.23) are solved by suitable routines for initial–value problems [97]. Two commonly used techniques are explicit Runge–Kutta methods [71] and modified equations methods [42]. The procedure of discretizing first in space is known as the method of lines, and allows us to focus on spatial discretizations.

Kreiss and Oliger introduced an important concept, number of grid points per wave length, in their pioneering work [63]. They analyzed the phase error for finite difference methods of order $q = 2, 4, 6$ for the advection equation, and derived a relation between the error tolerance ε, simulation time t, and the minimum number of grid points per wavelength M_q,

$$M_q \approx C_q \left(\frac{t}{\varepsilon}\right)^{1/q},$$

where the constant C_q depends on the order q of the method, but not t or ε. As the number of grid points per wavelength is proportional to the amount of computational work, we see that high–order methods are more efficient than low order methods if the simulation time is sufficiently long, or the error tolerance is sufficiently low. The same analysis is performed to the acoustic wave equation in [52], with the same conclusion obtained. This fact has motivated the development of high–order methods, i.e. numerical methods with rates of convergence higher than two.

In the following, we discuss the finite difference method, the finite element method and the discontinuous Galerkin method. For each method, we first address some generic properties and comment on the advantages and disadvantages from a general perspective. We then present different forms of the method, whose developments are usually motivated by overcoming some of the generic disadvantages. We conclude the section by discussing some other important numerical methods for wave propagation problems.

Finite difference methods

The finite difference method is one of the dominant approaches to solve partial differential equations numerically. Derivatives are approximated by difference

stencils using neighboring grid points. High–order finite difference stencils can be easily constructed in a one dimensional framework [37], and can be extended to higher dimensions through a dimension–by–dimension fashion. In general, such a procedure leads to a semi–discretized equation in the form of (2.23) with an identity matrix $\mathscr{M}$. Therefore, the semi–discretization is explicit, and we do not need to solve any system of linear equations. The finite difference method is conceptually simple and easy to implement.

From the above discussion we also see the disadvantages of the finite difference method in its basic form. The dimension–by–dimension structure makes the method difficult to use in domains with complex geometries, or problems with discontinuous parameters. In addition, when boundary conditions are non–periodic, it is not obvious how boundary conditions should be imposed so that the numerical solution converges with high order accuracy. To get convergence, we need consistency and stability. It is challenging to derive both stable and high–order accurate finite difference methods, especially for hyperbolic partial difference equations in the presence of boundaries and interfaces. For detailed discussions on stability and accuracy of finite difference methods, see [49, 50].

In the interior of a computation domain, a natural choice is central finite difference stencils. Close to boundaries, one–sided boundary stencils can be employed. From the accuracy point of view, it is desirable to use a boundary closure as accurate as the interior one. However, in many cases the resulting scheme is unstable, and we may have to accept a reduction of the order of accuracy of the boundary closure. One such example is the summation–by–parts finite difference method, which is central to this thesis and is used in Paper I–IV. We discuss it in more detail in Chapter 3.

Besides central finite difference stencils, compact finite differences of Padé type [29, 49] have been used to solve wave equations. For example, a fourth order accurate compact finite difference method in space and time is constructed in [28] for the acoustic wave equation. Comparing with a central finite difference method of the same order of accuracy, an advantage of a compact finite difference method is that the bandwidth is narrower and the coefficient of the leading truncation error is smaller. However, a banded system of linear equations must be solved at every time step, which complicates parallelization.

Waves often propagate in media with complex geometries, but a finite difference method can only be used in a rectangular–shaped domain with a Cartesian grid. There has been extensive work on the extension of finite difference methods for problems with complex geometries. One approach is to use a curvilinear grid to resolve the geometrical features of boundaries and interfaces. A computational domain is divided into subdomains, with each subdomain mapped to a reference domain. A common way is to partition the domain so that each subdomain is of quadrilateral shape, possibly with curved sides. With the unit square as a reference domain, a Cartesian grid in the unit square is mapped to each subdomain by transfinite interpolation [44]. At the same

time, the original equation must also be transformed, and the transformed equation often has a much more complicated form than the origin equation.

As an example, consider the acoustic wave equation in two space dimensions (x,y) with unit wave speed and density

$$u_{tt} = u_{xx} + u_{yy}.$$

Assuming the computational domain can be mapped smoothly to the unit square by transfinite interpolation, the transformed equation on a Cartesian grid (ξ,η) takes the form

$$Ju_{tt} = (\alpha u_\xi)_\xi + (\beta u_\xi)_\eta + (\beta u_\eta)_\xi + (\gamma u_\eta)_\eta.$$

The variable coefficients $\alpha(\xi,\eta)$, $\beta(\xi,\eta)$, $\gamma(\xi,\eta)$ and the Jacobian $J(\xi,\eta)$ depend on metric derivatives. We refer to [8] for a derivation of the transformation.

We see that even if the original equation has second derivatives with constant coefficients, the transformed equation has second derivatives with variable coefficients and mixed derivatives. When designing a finite difference method, it is important that the method solves the transformed equation in a stable and accurate manner. The finite difference methods developed in this thesis [106, 109] are of this kind.

To get an accurate solution on a curvilinear grid, the grid itself must be of high quality. In a high quality grid, the elements are not skewed too much. More specifically, the ratio between the longest side and the shortest side in an element is not too large, and ideally this ratio should be equal to one. In addition, the sizes of adjacent elements do not vary too much. These factors impose restrictions on the shape of the geometry. With an increased complexity of geometric features, advanced grid transformation techniques are needed [60].

For truly complex geometries arising from real–world applications, it may be impossible to find an appropriate domain partitioning strategy, grid generation and mapping. One naturally wants to embed the domain in a regular Cartesian grid, and use a so–called embedded method or immersed method. In the finite difference framework, Kreiss and his co–authors have developed second–order accurate methods for the acoustic wave equation subject to Dirichlet boundary conditions [66, 67], Neumann boundary conditions [68] and discontinuous coefficients [65]. A recent work [15] presents a fourth order embedded finite difference method of Padé type for the acoustic wave equation. These methods require artificial dissipations to ensure stability. A second order accurate scheme for Dirichlet problems is proposed in [6], where stability is guaranteed by constructing a symmetric negative semi–definite spatial operator.

Besides embedded techniques, a finite difference method on an overlapping grid is very attractive for problems with truly complex geometries. The

object–oriented toolkit, *Overture* [3], has been developed for solving partial differential equations with second and fourth order accurate finite difference methods on overlapping grids. The software supports curvilinear grids, adaptive mesh refinement and parallel computing. It provides simulations of a wide range of physical phenomena with moving geometries including compressible and incompressible flows, acoustic [19], elastic [9] and electromagnetic wave propagation [53]. In addition, stability and accuracy properties of these schemes are determined through a normal mode analysis.

Finite element methods

Another important numerical method to solve partial differential equations is the finite element method [101]. It is a Galerkin method characterized by a variational formulation, and has a solid mathematical foundation from functional analysis. The domain is discretized into non–overlapping elements, and in each element a set of polynomials are carefully selected as the trial functions. The numerical solution is a linear combination of the trial functions with the coefficients as the unknowns.

The element–based structure gives finite element methods an advantage over finite difference methods with respect to geometrical flexibility. Unstructured elements can be constructed to fill in the computational domain, and be aligned with parameter discontinuities. Boundary conditions are usually easier to impose than in the finite difference framework. Moreover, variable element sizes (h) and orders of accuracy (p) can be incorporated in the hp–finite element method [17].

The main disadvantage of finite element methods comparing with finite difference methods is that the semi–discretization (2.23) is implicit. The matrices $\mathscr{M}$ and $\mathscr{Q}$ are called mass matrix and stiffness matrix, respectively. The entries of $\mathscr{M}$ and $\mathscr{Q}$ are integrals of polynomials, and need to be computed either analytically or by quadrature. Due to the local coupling of elements, the mass matrix $\mathscr{M}$ has a banded structure, and we need to solve a banded system of linear equations.

An explicit space–time finite element method for the acoustic wave equation is developed in [96], and an implicit version is proposed in [56] for the elastic wave equation. Finite element methods have been implemented in several software libraries such as deal.II [1] and FEniCS [2].

The extended finite element method (XFEM) is an extension of the classical finite element method by enriching the solution space with extra functions [39]. The aim of enriching is to better capture certain apriori–known properties of the solution, for example the solution is discontinuous at a known location in space. With certain choices of the enriched functions, XFEM can be seen as a cut–finite element method (CutFEM) [21]. Similar to embedded methods in the finite difference framework, the computational domain is placed on a high quality background grid. This approach is attractive when high quality body–

fitted elements cannot be easily constructed because of complex geometries. CutFEM is applied successfully to the acoustic wave equation in [99].

Efforts have been made to combine advantages of finite difference method and finite element method. A finite difference method in Galerkin framework, the Galerkin difference method, has recently been developed in [18] for hyperbolic problems and applied to the acoustic wave equation. Accuracy analysis shows that the method possesses excellent dispersion property. In [20], a second order accurate hybrid method is used to solve the Maxwell's equation. Higher order hybrid methods can potentially be developed by the techniques in [62].

Discontinuous Galerkin methods

The discontinuous Galerkin method is a finite element method with piecewise continuous trial functions and solutions. It shares the advantages of the continuous finite element method, and adds on an important locality property. The mass matrix in the semi–discretization (2.23) is block–diagonal instead of banded, and can be inverted at low cost. In addition, the flexible choice of numerical fluxes can be utilized to reflect the dynamics of wave propagation. However, these attractive features come at a price. Since the numerical solutions are discontinuous across elements, degrees of freedom at element interfaces are duplicated, which increases the computational cost. For a general discussion of nodal discontinuous Galerkin methods, see the textbook [54].

Much work has been done in the discontinuous Galerkin framework for wave propagation problems. For the acoustic wave equation in the second–order form, a symmetric interior penalty discontinuous Galerkin method is developed in [46]. Energy stability is achieved by a proper choice of penalty parameters. The semi–discretization is in a very similar form to the SBP–SAT finite difference discretization. In [26], with the gradient of the solution introduced as additional variables, a local discontinuous Galerkin method is proposed. The auxiliary variable can be solved for locally, hence the name.

For the elastic wave equation, a staggered discontinuous Galerkin method is developed in [27] for the equation in the first–order velocity–stress formulation. The same formulation is approximated by an arbitrarily high–order discontinuous Galerkin method in [58] combined with arbitrary high–order derivatives (ADER) approach for time integration. The method is further extended in [59] to solve an acoustic–elastic coupled system in the same formulation. In a recent work [112] a discontinuous Galerkin method is proposed for an acoustic–elastic coupled system in the first–order velocity–strain formulation. A space–time finite element method is developed in [104] which incorporates time–discontinuous jumps.

An energy–based discontinuous Galerkin method is developed in [11] for general wave equations in the second–order form, and is specialized in [10] to the elastic wave equation. Inspired by the energy formulation of the governing equations, the temporal derivative of the solution is introduced as a new

variable. The technique is central to the second part of this thesis work, as we extend the method to solve acoustic–elastic coupled systems. We postpone a detailed discussion to Chapter 4.

A known drawback of a standard discontinuous Galerkin method is that the spectral radius grows quadratically with respect to the order of accuracy, unlike a linear growth for standard finite difference and finite element methods. This leads to a severe time–step restriction for stability when a very high–order spatial approximation and an explicit time integrator are used. Modified discontinuous Galerkin methods have been proposed [24, 110], which allow larger time steps than the original discontinuous Galerkin method.

The implementation of a high–order discontinuous Galerkin method could be challenging on domains with curved boundaries as one needs to take care of projection of data, quadrature for line, surface and volume integrations, transformation of non–rectangular geometries, and so on. A helpful textbook for efficient implementation of high–order Galerkin methods is [61].

Other numerical methods

There are many other numerical methods that have been used to solve wave propagation problems. Finite volume methods [72] are used in many computational fluid dynamics packages and nonlinear wave propagation problems, where conservations of physical quantities are highly important. Finite volume methods for linear and nonlinear hyperbolic systems, including acoustic and elastic wave equations, are implemented in the software package *Clawpack* [74].

The Hermite–Taylor method [43, 51] can be energy stable and arbitrarily high–order accurate. Moreover, the stability constraint on time step is independent of order of accuracy. Spatial derivatives at a grid point are approximated by using only information on that grid point, and time integration is achieved by using a staggered grid and Taylor series. The method has been used to simulate different physical problems including quantum mechanical waves [13]. A major drawback of Hermite–Taylor methods is the difficulty in imposing boundary conditions and representing complex geometries. One remedy is to design a hybrid method by coupling Hermite–Taylor method with discontinuous Galerkin method [25].

Radial basis function methods are a class of mesh free methods with scattered nodes in space, where a radial basis function is associated with each node. Geometrical features of the computational domain can be represented accurately by placing nodes on boundaries, and spectral convergence can be obtained when problems are sufficiently regular. The methods are powerful in geoscience modeling of weather predictions and seismic waves [38].

3. The summation–by–parts finite difference method

To solve wave propagation problems, we in general need operators to approximate three derivatives in one space dimension:

- first derivative $D_1 \approx \frac{\partial}{\partial x}$,
- second derivative with constant coefficient $D_2 \approx \frac{\partial^2}{\partial x^2}$,
- second derivative with variable coefficient $D_2^{(b)} \approx \frac{\partial}{\partial x}\left(b(x)\frac{\partial}{\partial x}\right)$, where $b(x)$ is a known, smooth function.

Operators for the approximation of derivatives in multi–dimensions can be constructed by using tensor products. To discuss summation–by–parts properties, we focus on the first derivative approximation in one space dimension.

Summation–by–parts property

In calculus, the integration–by–parts formula states

$$\int_0^1 uv_x dx = uv|_0^1 - \int_0^1 u_x v dx, \tag{3.1}$$

for smooth, real–valued functions $u(x), v(x)$ on [0,1].

Summation–by–parts (SBP) is the discrete counterpart of integration–by–parts. To see their relation, we discretize the domain [0,1] uniformly with n points as $x_j = (j-1)h,\ j = 1, \cdots, n$, where $h = 1/(n-1)$ is the grid spacing. Let the restrictions of $u(x), v(x)$ to the grid be $n \times 1$ vectors

$$\boldsymbol{u} = [u(x_1), \cdots, u(x_n)]^T, \quad \boldsymbol{v} = [v(x_1), \cdots, v(x_n)]^T.$$

There are two ingredients for a discretization of (3.1):

- A difference operator D_1: $(D_1\boldsymbol{u})_j \approx u_x(x_j)$,
- A quadrature $\boldsymbol{u}^T H \boldsymbol{v} \approx \int_0^1 uv dx$.

The operator H is symmetric positive definite, and defines a discrete norm $\|\boldsymbol{u}\|_H^2 = \boldsymbol{u}^T H \boldsymbol{u} \approx \int_0^1 u^2 dx$.

An analogue of (3.1) can then be written as

$$\boldsymbol{u}^T H D_1 \boldsymbol{v} = \boldsymbol{u}^T E_x \boldsymbol{v} - (D_1\boldsymbol{u})^T H \boldsymbol{v},$$

where $E_x = \mathrm{diag}(-1, 0, \cdots, 0, 1)$ is an extract operator. The discrete formula is equivalent to

$$HD_1 + (HD_1)^T = E_x, \tag{3.2}$$

Table 3.1. *For the diagonal–norm SBP operators constructed in [69, 75, 82, 100], the relations between order of accuracy and number of boundary points are listed below.*

$2r$: Interior order of accuracy	r: Boundary order of accuracy	n_b: Number of boundary points
2	1	1
4	2	4
6	3	6
8	4	8

which is the SBP property for the first derivative operator. For any specific grid with n points, the operators can be represented by matrices of size n.

We note that E_x has only two non–zero components at two corners. At interior points an obvious choice is to use standard central difference stencils for D_1, and the weights of a standard discrete L_2 norm for H. The interior of H is then diagonal with grid spacing h as the diagonal elements. The order of accuracy of D_1 at interior points is even, denoted by $2r$, because of the centered structure. However, it is clear that close to boundaries both H and D_1 must be modified. Two questions arise:

- How do we modify H and D_1 at boundaries so that the SBP property (3.2) is satisfied?
- What is the order of accuracy of D_1 at boundaries?

Development of summation–by–parts finite difference operators

Kreiss and Scherer answered these questions in [69]. They found out that H can actually be diagonal, with modified weights close to boundaries. However, the order of accuracy of D_1 at those boundary points can at most be r, i.e. half the order of accuracy at interior points. This kind of operators are referred to as diagonal–norm SBP operators. Block–norm SBP operators have an order of accuracy $2r-1$ at boundary points, where H has a block structure at two boundaries. In [69], both diagonal–norm and block–norm first derivative SBP operators D_1 are constructed for $r = 1,2,3,4$. These operators are further discussed in [70, 100].

In Table 3.1, we list the order of accuracy and the number of boundary points n_b for $r = 1,2,3,4$, which suggests that the number of boundary points grows linearly with order of accuracy. However, when Mattsson and Almquist constructed D_1 with $r = 5$ they had to use 11 boundary points [77]. In [7], Albin and Klarmann performed a careful analysis on the minimum number of boundary points, n_b, for a given order of accuracy, r. Their results show that n_b grows quickly for large r. For example, when $r = 15$, the minimum number of boundary points is 71. SBP operators with such a large number of boundary points are hardly useful for practical computations.

Applying D_1 twice, D_1D_1, approximates second derivative $\partial^2/\partial x^2$. However, there are two drawbacks of using D_1D_1: 1) the interior stencil of D_1D_1 is wider than the standard central finite difference stencil of the same accuracy, 2) the order of accuracy at boundaries is reduced to $r-1$. These two factors could lead to suboptimal performance of the numerical method. In [82], second derivative SBP operators $D_2 \approx \partial^2/\partial x^2$ are constructed with both diagonal and block norms for $r = 1,2,3,4$. These operators use standard central finite differences as interior stencils, and have the same number of boundary points as D_1 shown in Table 3.1.

The second derivative with variable coefficient $\partial/\partial x(b(x)\partial/\partial x)$ appears in wave propagation problems in inhomogeneous media. A curvilinear mapping of a non–rectangular domain also introduces variable coefficients. In both cases, the variable coefficient is strictly positive $b(x) > 0$. The corresponding SBP operators $D_2^{(b)} \approx \partial/\partial x(b(x)\partial/\partial x)$ are constructed in [75] with diagonal–norms for $r = 1,2,3$.

Block–norm SBP operators have better accuracy property than diagonal–norm operators, but are not often used in computations. This is because when block–norm operators are used for problems with variable coefficients, from material parameters or curvilinear mapping, the numerical scheme is not provably stable, and in many cases is indeed unstable. In a recent work [77], artificial dissipations are used to stablize the discretization with block–norm SBP operators.

Efforts have been made towards improved order of accuracy at boundaries of first derivative SBP operators. In [78], by using a non–equidistant grid distribution close to boundaries, the coefficient of the leading order error is minimized. Even though the formal order of accuracy is not improved, the gain the accuracy in numerical experiments is enormous. A similar approach is used in [52]. With one or two non–equidistant grid points near the boundary, the order of accuracy is equally high at the boundary and in the interior. However, the scheme does not possess an SBP property, thus an energy estimate is difficult to derive. In [31], corner–corrected SBP operators are constructed, where the order of accuracy at boundaries is the same as in the interior. Recently developed upwind SBP operators [76] also have improved accuracy.

To improve geometrical flexibility, in [30] generalized SBP operators are constructed on non–uniform grids, and boundaries do not need to conform with the grid. This technique is extended to multi–dimensional simplices in [55], where the multi–dimensional operators are not a simple extension of one dimensional operators by tensor products.

All the above mentioned works concern spatial discretizations. Recent developments also extend the SBP concepts to time domains for initial–value problems [73, 86, 87].

Other numerical methods in summation–by–parts form
Summation–by–parts properties were initially associated with finite difference methods. However, recent developments show that some other numerical methods can also be written in a summation–by–parts form. In [35, 36], a finite volume method with a summation–by–parts property is used to solve conservation laws. In [85], a second–order accurate finite volume method is shown to have a multi–dimensional summation–by–parts property even on unstructured meshes. The multi–dimensional triangular–element summation–by–parts operators constructed in [55] bear similarities with finite element methods. A discontinuous Galerkin collocation spectral element method with Gauss–Lobatto points also satisfies a summation–by–parts principle [40]. Another discontinuous Galerkin method on a split form with a summation–by–parts property is developed for the compressible Euler equations [41].

3.1 Stability analysis

Continuous analysis
We consider the acoustic wave equation in one space dimension with homogeneous Neumann boundary conditions

$$u_{tt} = u_{xx} + F, \quad x \in [0,1], \quad t \geq 0, \tag{3.3}$$
$$u(x,0) = u_0(x), \quad u_t(x,0) = u_1(x), \tag{3.4}$$
$$u_x(0,t) = u_x(1,t) = 0. \tag{3.5}$$

Multiplying equation (3.3) by u_t and integrate in x from 0 to 1, we obtain

$$\int_0^1 u_t u_{tt} dx = \int_0^1 u_t u_{xx} dx + \int_0^1 u_t F dx. \tag{3.6}$$

We denote the L_2 norm of u by $\|u\|^2 = \int_0^1 u^2 dx$, and recognize that the term on the left–hand side of (3.6) is

$$\int_0^1 u_t u_{tt} dx = \frac{1}{2}\frac{d}{dt}\|u_t\|^2, \tag{3.7}$$

and the integration–by–parts principle leads the first term of the right–hand side of (3.6) to

$$\int_0^1 u_t u_{xx} dx = u_t u_x|_0^1 - \int_0^1 u_x u_{tx} dx = u_t u_x|_0^1 - \frac{1}{2}\frac{d}{dt}\int_0^1 (u_x)^2 dx. \tag{3.8}$$

We note that $u_t u_x|_0^1 = 0$ because of the boundary condition (3.5). Thus, (3.6) is equivalent to

$$\frac{d}{dt}\int_0^1 [(u_t)^2 + (u_x)^2] dx = 2\int_0^1 u_t F dx. \tag{3.9}$$

We associate equation (3.3) with an energy $\|u\|_E^2 = \int_0^1 [(u_t)^2 + (u_x)^2]dx$, where the energy norm $\|u\|_E$ is a semi–norm of u. By Cauchy–Schwarz inequality, (3.9) becomes

$$\frac{d}{dt}\|u\|_E^2 = 2\|u\|_E \frac{d}{dt}\|u\|_E \leq 2\|u_t\|\|F\| \leq 2\|u\|_E\|F\|.$$

Integrating in time gives the final energy estimate

$$\|u\|_E \leq \|u(\cdot,0)\|_E + \int_0^t \|F(\cdot,\hat{t})\|d\hat{t}.$$

The bound on the energy $\|u\|_E$ is determined by the initial data (3.4) and the forcing term F. The above procedure, known as the energy method, proves that the energy of equation (3.3)–(3.5) is bounded by the data. As a consequence, the growth rate of the solution u is limited by the energy estimate.

We wish to construct a difference operator so that the energy associated with the semi–discretization is bounded in the same way as the corresponding energy of the continuous equation. In other words, there should be no growth of the numerical solution that is not present in the continuous problem. We denote such a discretization time stable. Time stable methods are important for long time simulations of wave propagation. We note the key in obtaining an energy estimate is the integration–by–parts principle.

Semi–discrete analysis

We now approximate u_{xx} in (3.3) by an SBP operator D_2, and investigate if an energy estimate in the discrete setting is possible. It may seem surprising at first glance that the SBP property itself does not lead to an energy estimate. The reason is that in the continuous setting the boundary term in (3.8) vanishes because of the boundary condition (3.5), but the corresponding discrete boundary term does not automatically vanish in the discrete energy estimate. The existence of a discrete energy estimate depends on how boundary conditions are imposed.

Several techniques have been proposed for imposing boundary conditions in the SBP finite difference framework. The projection method can be used to impose boundary conditions in a strong sense [88, 89]. However, the method cannot be easily extended to problems with complex geometries. The ghost point method can also be used to imposed boundary conditions strongly, and has been used in many second–order accurate finite difference and finite volume methods. A fourth–order accurate SBP finite difference method using ghost points is implemented in the open code SW4 [4], which solves elastic wave equations for seismic modeling. SW4 is capable to provide simulations in three space dimensions on Cartesian [98] and curvilinear grids [94] with free surface boundaries. In addition, far–field boundaries are treated by using absorbing boundary conditions [91] and a super–grid technique [93]. Discretizations with singular point source [90, 92] and non–conforming interfaces

[92] are also developed. The stencils on the ghost points are carefully chosen to maintain stability and accuracy.

The simultaneous–approximation–term (SAT) method [22, 23] is very popular in the SBP framework for imposing boundary conditions. Here, boundary conditions are imposed weakly by adding penalty terms to the semi–discretization, which is similar to how boundary conditions are imposed in the Nitsche's finite element method and the discontinuous Galerkin method.

The above techniques can also be used to impose interface conditions between two subdomains. No matter which method is used, it is important to be able to derive a discrete energy estimate. In this thesis, the SAT method is exclusively used in the finite difference framework because of its simplicity in multi–dimensional problems. Below we demonstrate how to obtain a discrete energy estimate by using an SBP–SAT finite difference method.

Let $\boldsymbol{v}$ be the discrete solution vector. As is shown in [82], the second derivative SBP operator has a structure

$$D_2 = H^{-1}(-M + E_x S),$$

where H is positive definite, M is symmetric positive semi–definite, the first and last row of S approximate first derivative at boundaries, and the extractor operator $E_x = \text{diag}(-1, 0, \cdots, 0, 1)$. Note that H and M define a discrete L_2 norm and semi–norm, respectively.

The semi–discretization reads

$$\begin{aligned} \boldsymbol{v}_{tt} &= \overbrace{D_2\boldsymbol{v}}^{\text{SBP}} + \overbrace{\tau H^{-1}(E_x S\boldsymbol{v} - \boldsymbol{0})}^{\text{SAT}} + \mathscr{F} \\ &= H^{-1}(-M + E_x S)\boldsymbol{v} + \tau H^{-1} E_x S\boldsymbol{v} + \mathscr{F} \\ &= -H^{-1}M\boldsymbol{v} + (1+\tau)H^{-1}E_x S\boldsymbol{v} + \mathscr{F}, \end{aligned}$$

where $\mathscr{F}(t)$ is the restriction of the forcing $F(x,t)$ onto the grid. We multiply $2\boldsymbol{v}_t^T H$ on both sides. After rearranging terms, we obtain

$$2\boldsymbol{v}_t^T H\boldsymbol{v}_{tt} + 2\boldsymbol{v}_t^T M\boldsymbol{v} = 2(1+\tau)\boldsymbol{v}_t^T E_x S\boldsymbol{v} + 2\boldsymbol{v}_t^T H\mathscr{F}. \tag{3.10}$$

We note that the left–hand side can be written as

$$\frac{d}{dt}(\boldsymbol{v}_t^T H\boldsymbol{v}_t + \boldsymbol{v}^T M\boldsymbol{v}),$$

which is the discrete analogue of the left–hand side of (3.9) with a discrete energy $\|\boldsymbol{v}\|_{\boldsymbol{E}}^2 = \boldsymbol{v}_t^T H\boldsymbol{v}_t + \boldsymbol{v}^T M\boldsymbol{v}$. To also get an analogue of the right–hand side of (3.9), we need the first term of (3.10) to vanish, which can be achieved by the choice $\tau = -1$. The semi–discretization then becomes

$$\boldsymbol{v}_{tt} = -H^{-1}M\boldsymbol{v} + \mathscr{F}. \tag{3.11}$$

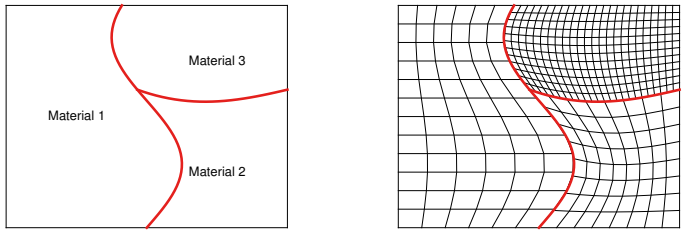

(a) *(b)*

Figure 3.1. Non–conforming interfaces

A discrete energy estimate follows in the same way as in the continuous case,

$$\|\boldsymbol{v}\|_E \leq \|\boldsymbol{v}(0)\|_{\boldsymbol{E}} + \int_0^t \|\mathscr{F}(\hat{t})\|_H d\hat{t}.$$

Therefore, the possible growth of the numerical solution $\boldsymbol{v}$ is limited by the discrete energy estimate, and is determined by the data of the continuous problem.

Other boundary and interface conditions in the SBP–SAT framework
The SBP–SAT finite difference method is used to solve the acoustic wave equation with Dirichlet boundary conditions [12, 81], Neumann boundary conditions [81], and discontinuous material parameters [80]. The technique is extended to curvilinear grids for multi–dimensional problems in [105].

In an inhomogeneous medium, the wave speed varies in space. For a given frequency, the wave length is shorter in the region where the wave speed is smaller. According to the theory in [63], for computational efficiency the number of grid points in each subdomain should be chosen according to the wave length therein. This naturally leads to non–conforming grid interfaces. For example, the domain shown in Figure 3.1a consists of three media and the mesh shown in Figure 3.1b is an illustration of non–conforming grid interfaces.

In Paper I [109], we develop SBP finite difference methods for acoustic wave propagation described in Problem 1. Particular emphasize is placed on numerical interface coupling with a general geometrical configuration as shown in Figure 3.1b. Adjacent subdomains are connected by interpolation operators [62, 79] and the SAT method. The penalty terms in the SAT method are constructed as a straightforward generalization of those used for conforming interfaces [105]. In this case, energy stability can only be proved under a rather restrictive condition on the interpolation operators. It is numerically verified that only some low order accurate interpolation operators satisfy the needed assumption. In Paper II [106], we construct new penalty terms in the SAT method for interface coupling. The resulting numerical scheme is energy

stable without the restrictive condition required in the scheme developed in Paper I, and allows for higher–order accuracy.

The elastic wave equation with free surface boundary conditions is a challenging problem. Recent development includes second order accurate methods [14, 84] and higher–order methods [33]. In addition, high–order methods have also been developed for elastic wave propagation problems with interfaces [34]. For general discussions on SBP–SAT finite difference methods, we refer to the two review papers [32, 102].

3.2 Accuracy analysis

As discussed in the preceding section, the commonly used diagonal–norm SBP operators have an interior order of accuracy $2r$ because of the centered stencils. At a few points close to boundaries, the stencils are modified to satisfy an SBP property, and the order of accuracy drops to r. A natural question is what is the rate of convergence of the numerical scheme. At first glance, the rate of convergence seems to be r dictated by the large truncation error at boundary points. However, numerical experiments often show a better result, where a numerical solution converges at a rate higher than r. This can be partially explained by the fact that the number of boundary points is independent of grid spacing, see Table 3.1. As a consequence, when the grid spacing approaches zero, the effect of large truncation errors at a few boundary points to the overall rate of convergence may be weakened.

Convergence analysis has been a long–standing research topic. When using a stable numerical method to solve a linear problem, a straightforward way to analyze rate of convergence is to apply the energy method to the error equation. As an example, consider the stable SBP approximation (3.11) with the penalty parameter $\tau = -1$. We define the pointwise error vector $\boldsymbol{e} = [e_1, \cdots, e_n]^T$ where $e_j = u(x_j) - v_j$ for $j = 1, \cdots, n$. The pointwise error satisfies the semi–discretization (3.11) with the truncation error $\mathscr{T}$ as a forcing

$$\boldsymbol{e}_{tt} = -H^{-1}M\boldsymbol{e} + \mathscr{T}, \tag{3.12}$$

where the truncation error vector has a structure

$$\mathscr{T} = [\underbrace{\mathscr{O}(h^r), \cdots, \mathscr{O}(h^r)}_{n_b}, \underbrace{\mathscr{O}(h^{2r}), \cdots, \cdots, \cdots, \mathscr{O}(h^{2r})}_{n_i}, \underbrace{\mathscr{O}(h^r), \cdots, \mathscr{O}(h^r)}_{n_b}]^T.$$

It is important to note that the number of boundary points n_b is independent of grid spacing, and the number of interior points n_i increases as grid is refined. At the limit when grid spacing goes to zero, there are still just a few boundary points but infinitely many interior points. We refer to the truncation errors $\mathscr{O}(h^r)$ on the boundary points as boundary truncation errors, and say that the

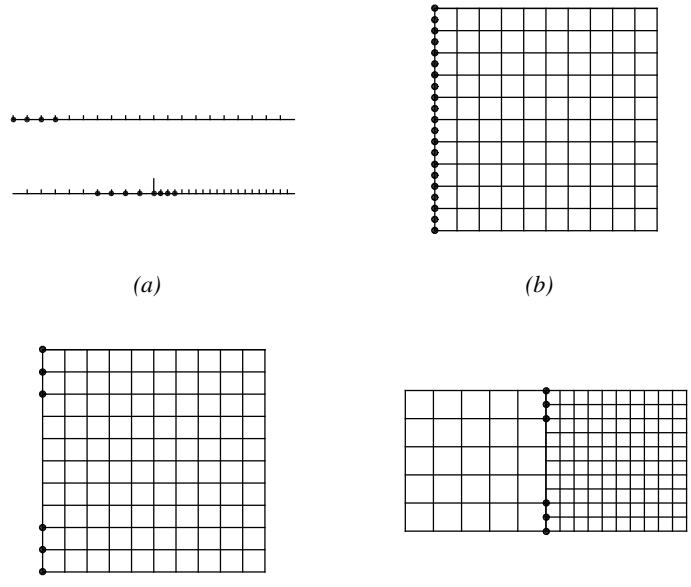

Figure 3.2. Grid points with a large truncation error are marked by a solid circle. The truncation error elsewhere is assumed to be much smaller.

boundary truncation errors are localized. More precisely, they are localized to a space one dimension lower than the computational domain.

This scenario can be generalized to multi–dimensions. In particular, for two dimensional problems the boundary truncation errors are localized along boundaries. An additional scenario, which does not exist in one dimensional problems, is that the dominating truncation errors are localized at a fixed number of grid points, i.e. localized to a space two dimensions lower than the computational domain. This is a case typically found in the multi–block finite difference framework when non–conforming grid interfaces are present. In particular, the method developed in [109] has a truncation error $\mathcal{O}(h^{2r})$ in the interior of the computational domain, but $\mathcal{O}(h^{r-2})$ at a few points near the corner of a non–conforming interface. Experiments demonstrate that the solution in general converges at a rate $\mathcal{O}(h^{r+1})$, i.e. a gain of three orders in convergence.

The third contribution of this thesis is devoted to a better understanding of how the dominating truncation errors, typically localized to a space whose dimension is lower than the computational domain, affect the overall rate of convergence of the numerical scheme. We in particular consider stable finite difference schemes applied to the acoustic wave equation in one and two space dimensions. The mathematical problem is formulated as follows.

Problem 3. *The acoustic wave equation*

$$u_{tt} = \nabla \cdot \nabla u$$

is solved on a Cartesian grid by a stable finite difference method. We consider the following three cases.

- *The one dimensional problem with Dirichlet and Neumann boundary conditions, and the problem with a grid interface, where boundary truncation errors are localized on a few grid points shown in Figure 3.2a.*
- *A two dimensional problem where boundary truncation errors are localized on an entire boundary shown in Figure 3.2b.*
- *A two dimensional problem where boundary truncation errors are localized only on a few grid points at a corner shown in Figure 3.2c.*

We aim at determining the effect of boundary truncation errors in the above three cases on the overall rate of convergence of the numerical scheme.

We note that the last case in Problem 3 is a simplified model of a problem with a non–conforming grid interface shown in Figure 3.2d.

The energy method

The error equation (3.12) is linear, we can therefore decompose $\mathscr{T}$ into two parts: the interior truncation error of order $\mathscr{O}(h^{2r})$ and the boundary truncation error of order $\mathscr{O}(h^2)$. We have

$$\boldsymbol{e}^i_{tt} = -H^{-1}M\boldsymbol{e}^i + \mathscr{T}^i, \tag{3.13}$$

$$\boldsymbol{e}^b_{tt} = -H^{-1}M\boldsymbol{e}^b + \mathscr{T}^b, \tag{3.14}$$

where

$$\mathscr{T}^i = [\underbrace{0,\cdots,0}_{n_b},\underbrace{\mathscr{O}(h^{2r}),\cdots,\cdots,\cdots,\mathscr{O}(h^{2r})}_{n_i},\underbrace{0,\cdots,0}_{n_b}]^T,$$

$$\mathscr{T}^b = [\underbrace{\mathscr{O}(h^r),\cdots,\mathscr{O}(h^r)}_{n_b},\underbrace{0,\cdots,\cdots,\cdots,0}_{n_i},\underbrace{\mathscr{O}(h^r),\cdots,\mathscr{O}(h^r)}_{n_b}]^T.$$

We note that $\mathscr{T} = \mathscr{T}^i + \mathscr{T}^b$ and $\boldsymbol{e} = \boldsymbol{e}^i + \boldsymbol{e}^b$, and the initial data of (3.13) and (3.14) are zero. The two equations (3.13) and (3.14) are in exactly the same form as the semi–discretization (3.11). Therefore, the discrete energy estimates for (3.13) and (3.14) are

$$\|\boldsymbol{e}^i\|_{\boldsymbol{E}} \le \int_0^t \|\mathscr{T}^i(\hat{t})\|_H d\hat{t} \sim \mathscr{O}(h^{2r}),$$

$$\|\boldsymbol{e}^b\|_{\boldsymbol{E}} \le \int_0^t \|\mathscr{T}^b(\hat{t})\|_H d\hat{t} \sim \mathscr{O}(h^{r+1/2}).$$

Since $2r > r+1/2$ for any positive integer r, the above estimates show that the total error $\boldsymbol{e}$ in the discrete energy norm goes to zero at a rate $r+1/2$. In

other words, we *gain a half order in convergence*. This result is valid as long as there is an energy estimate of the semi–discretization. As suggested by many numerical experiments, the half order gain in convergence is not sharp and more analysis is needed to obtain sharp estimates. A more careful energy analysis to the heat equation shows that the gain in convergence can be one and half orders, though numerical experiments show a gain of two orders [5].

The normal mode analysis

The normal mode analysis turns out to be a more powerful tool for analysis of rate of convergence. The principal idea is to perform a Laplace transformation of (3.14) in time, which converts the ordinary differential equations to a set of difference equations. In the interior the finite difference stencils are repeated, and a general solution of the difference equations can be obtained by solving a characteristic equation. A boundary system is then formed by substituting the general solution into the boundary equation. The crucial part is to estimate the solution to the boundary system. This estimate is often dominated by the behavior of the Laplace transformed errors close to the imaginary axis. A stable scheme guarantees that the boundary system is non–singular in the right half–plane in Laplace space, but the boundary system can be singular on the imaginary axis. The estimates in the Laplace space are transformed back to the physical space by Parseval's relation.

Gustafsson performed normal mode analysis for fully discrete schemes applied to first–order hyperbolic systems in [47], and gave technical assumptions under which the gain in convergence is one order. The results from [47] are generalized to mixed initial–boundary value problems with first–order temporal derivative in [48]. Both works concern problems in one space dimension.

As a rule of thumb, the gain in convergence for a stable finite difference method is equal to the highest order of spatial derivatives. This is straightforwardly true if in the normal mode analysis, the boundary system in the Laplace space is non–singular on the imaginary axis. We have found the rule of thumb does not hold for the acoustic wave equation with certain boundary conditions. The gain in convergence is not always two, but depends on boundary conditions and how they are imposed.

In Paper III [107], we consider the acoustic wave equation in one space dimension, i.e. the first item in Problem 3. For problems with Dirichlet boundary conditions and interfaces, a normal mode analysis shows that the overall rate of convergence depends on the free penalty parameter in the semi–discretization. Different choices could lead to a suboptimal convergence with only a half order gain, or a super–convergence with a two and half orders gain.

In Paper IV [108], we extend the convergence analysis to the acoustic wave equation in two space dimensions. A diagonalization procedure decomposes a two dimensional problem to many one dimensional problems of the same type as the one analyzed in Paper III [107]. A normal mode analysis is performed to each decomposed problem, and the results are then combined to obtain

the final estimate for the original two dimensional problem. In particular, we consider two cases, item two and three in Problem 3. We find that when a large truncation error is located along an entire boundary, the gain in convergence is determined by the corresponding one dimensional problem. When a large truncation error is only localzed on a few grid points, an extra one order can be gained in convergence.

We have conducted numerical experiments to verify that the theoretical accuracy analyses in Paper III and IV are sharp.

4. The energy–based discontinuous Galerkin method

In Section 3.1, an energy estimate is derived for the wave equation in one space dimension. The same procedure can be applied to the equation in its general form (2.4), which has a continuous energy

$$E_a = \frac{1}{2}\int_\Omega \frac{1}{\rho c^2}(p_t)^2 + \frac{1}{\rho}\nabla p \cdot \nabla p. \tag{4.1}$$

The change of energy in time is determined by the boundary contributions

$$\frac{dE_a}{dt} = \int_{\partial\Omega} \frac{1}{\rho} p_t (\nabla p \cdot \boldsymbol{n}),$$

where $\boldsymbol{n}$ is the outward pointing normal of $\partial\Omega$. The elastic wave equation (2.13) has a similar energy whose change in time is also determined by boundary contributions. Based on this fact, an energy–based discontinuous Galerkin method was developed in [11] for the spatial discretization of wave equations in the second–order form. The method is applicable to both the acoustic wave equation and the elastic wave equation.

Below we use the acoustic wave equation (2.4) with Dirichlet boundary conditions as an example to show the main idea of the method. With a new variable $w = p_t$, the governing equation becomes

$$p_t = w, \tag{4.2}$$

$$\frac{1}{\rho c^2} w_t = \nabla \cdot \left(\frac{1}{\rho}\nabla p\right) + \frac{F}{\rho}, \tag{4.3}$$

with the Dirichlet boundary condition

$$p = g(t) \quad \partial\Omega.$$

The domain is discretized by a mesh $\mathscr{T}_h$ into non–overlapping quadrilaterals $\Omega = \cup\Omega_j$, possibly with curved sides to fit the domain. We approximate the solution p and w in the finite element space

$$V_p^h := \{\phi_p : \phi_p|_{\Omega_j} \in \mathscr{P}^{q_p}(\Omega_j), \forall \Omega_j \in \mathscr{T}_h\},$$

and

$$V_w^h := \{\phi_w : \phi_w|_{\Omega_j} \in \mathscr{P}^{q_w}(\Omega_j), \forall \Omega_j \in \mathscr{T}_h\},$$

respectively. The space $\mathscr{P}^{q_p}(\Omega_j)$ consists of tensor product polynomials of degree at most q_p in each variable defined in Ω_j.

On each element Ω_j, we test equation (4.2) with a non–standard test function $\nabla\cdot(\frac{1}{\rho}\nabla\phi_p)$, and equation (4.3) with a standard test function ϕ_w,

$$\int_{\Omega_j}(p_t^h - w^h)\nabla\cdot\left(\frac{1}{\rho}\nabla\phi_p\right) = 0,$$
$$\int_{\Omega_j}\left(\frac{1}{\rho c^2}w_t^h - \nabla\cdot\left(\frac{1}{\rho}\nabla p^h\right) - \frac{F}{\rho}\right)\phi_w = 0,$$

where p^h and w^h are approximations of p and w, respectively. Integration by parts leads to

$$\int_{\Omega_j}\nabla(p_t^h - w^h)\cdot\left(\frac{1}{\rho}\nabla\phi_p\right) = \int_{\partial\Omega_j}\frac{1}{\rho}(p_t^h - w^h)\nabla\phi_p\cdot\mathbf{n_j}, \tag{4.4}$$
$$\int_{\Omega_j}\frac{1}{\rho c^2}w_t^h\phi_w + \frac{1}{\rho}\nabla p^h\cdot\nabla\phi_w = \int_{\partial\Omega_j}\frac{1}{\rho}(\nabla p^h\cdot\mathbf{n_j})\phi_w + \frac{F}{\rho}\phi_w. \tag{4.5}$$

Next, we replace p_t^h, $\nabla p^h\cdot\mathbf{n_j}$ by w^*, $(\nabla p\cdot\mathbf{n_j})^*$ on the right–hand side of (4.4), (4.5), respectively, and obtain

$$\int_{\Omega_j}\nabla(p_t^h - w^h)\cdot\left(\frac{1}{\rho}\nabla\phi_p\right) = \int_{\partial\Omega_j}\frac{1}{\rho}(w^* - w^h)\nabla\phi_p\cdot\mathbf{n_j}, \tag{4.6}$$
$$\int_{\Omega_j}\frac{1}{\rho c^2}w_t^h\phi_w + \frac{1}{\rho}\nabla p^h\cdot\nabla\phi_w = \int_{\partial\Omega_j}\frac{1}{\rho}(\nabla p\cdot\mathbf{n_j})^*\phi_w + \frac{F}{\rho}\phi_w. \tag{4.7}$$

When the test function ϕ_p is linear, equation (4.6) trivially reduces to $0=0$, but can be replaced by an independent equation

$$\int_{\Omega_j}(p_t^h - w^h) = 0.$$

The star variables w^* and $(\nabla p\cdot\mathbf{n_j})^*$ are numerical fluxes, and are crucial for the stability and accuracy properties of the semi–discretization. They are determined in the stability analysis so that an energy estimate can be obtained.

We consider numerical fluxes in two cases: when $\partial\Omega_j$ is an interface between two elements, and when $\partial\Omega_j$ is on the boundary of Ω. In the first case, let two elements Ω_1 and Ω_2 share an interface Γ_{12} as shown in Figure 4.1. Then the numerical fluxes on Γ_{12} in a general form are given by

$$w^* = \alpha w_1 + (1-\alpha w_2) - \tau(\nabla p_1\cdot\mathbf{n_1} + \nabla p_2\cdot\mathbf{n_2})$$
$$(\nabla p\cdot\mathbf{n_1})^* = (\alpha\nabla p_2 + (1-\alpha)\nabla p_1))\cdot\mathbf{n_1} - \beta(w_1 - w_2),$$
$$(\nabla p\cdot\mathbf{n_2})^* = (\alpha\nabla p_2 + (1-\alpha)\nabla p_1))\cdot\mathbf{n_2} - \beta(w_2 - w_1).$$

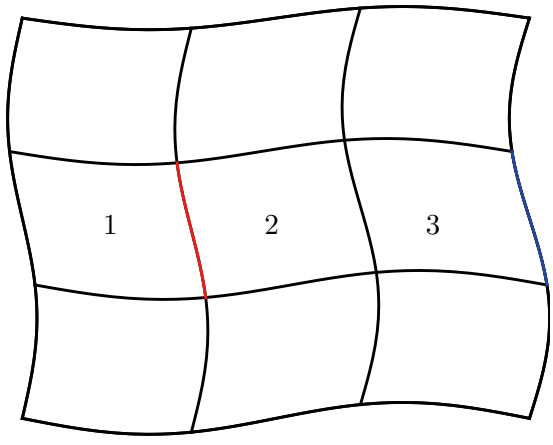

Figure 4.1. A grid consists of nine elements. The interface between the elements 1 and 2 in red is an interior face, and the right side of the element 3 in blue is a boundary face.

When $\tau = \beta = 0$, an energy conserving discretization is obtained. In this case, $\alpha = 0.5$ corresponds to central fluxes, and $\alpha = 0$ or 1 corresponds to alternating fluxes. Artificial dissipations can be easily added by choosing $\beta > 0$ or $\tau > 0$. The second case concerns how the Dirichlet boundary condition is imposed. We consider the element 3 shown in Figure 4.1. At the right boundary, we set

$$w^* = \frac{d}{dt} g(t) \quad \text{and} \quad (\nabla p \cdot \mathbf{n_3})^* = \nabla p \cdot \mathbf{n_3}.$$

The above numerical fluxes lead to an energy–stable semi–discretization. We note that the flux parameters are mesh–independent. High–order approximations can be achieved by using high–order polynomials in the finite element spaces V_p^h and V_w^h. In addition, numerical experiments [11, 10] demonstrate that optimal convergence rates are obtained with both energy–conserving and dissipative discretizations. We remark that the new variable $w = p_t$ in (4.2) is naturally related to the continuous energy (4.1), and does not introduce additional computational work when using a Runge–Kutta type time integrator.

In Paper V [16], we use the energy–based discontinuous Galerkin method to simulate wave propagation in a fluid–solid coupled medium as described in Problem 2. Wave propagation in the fluid is modeled by the acoustic wave equation in terms of velocity potential. In the solid, the elastic wave equation in the second–order displacement formulation is used as the governing equation. Particular emphasize is placed on numerical coupling of the interface between the acoustic medium and the elastic medium.

5. Outlook

The focus of this thesis is on the development and analysis of numerical methods for second–order hyperbolic partial differential equations. There are many exciting research topics that can be seen as extensions of the current work.

In Paper I and II, a high–order finite difference method is developed on curvilinear grids with non–conforming interfaces. The method is specialized to the acoustic wave equation. A natural extension is to use the method to solve the elastic wave equation. Seismic waves propagate in the earth that has a non–flat, layered structure. Due to inhomogeneity, an incoming wave with a given frequency will have different wave lengths in the earth layers. For computational efficiency, a uniform number of grid points per wave length should be used. It then naturally leads to non–conforming grid interfaces, and the technique developed in Paper I and II is well–suited for such problems. Another direction of future research is to consider seismic wave propagation in a domain with cracks. The difficulty here is that an extremely fine grid is needed to fully resolve the crack structures. For computational efficiency, a multiscale approach is expected to be more appropriate. Alternatively, one can model the cracks as boundary conditions based on the physical properties.

In Paper III and IV, the normal mode analysis is used to derive error estimates for a class of finite difference methods for the wave equation in one and two space dimensions. The results highlight the strong ability of the normal mode analysis in deriving sharp error estimates. Potentially the technique can be used for systems of partial differential equations, such as the elastic wave equation. When the computational domain consists of two elastic media in contact, an SBP–SAT finite difference method exhibits a higher than expected rate of convergence [34]. It is interesting to perform a normal mode analysis for this problem, and understand the superconvergence phenomenon.

I Paper V, an energy–based discontinuous Galerkin method is used for wave propagation problems in fluid–solid coupled domains. An exciting extension to this work is to consider deforming domains, for example, a solid object moving and deforming in a fluid. To capture the movement, re–meshing is needed in every time step with a standard discontinuous Galerkin method. This is in many cases infeasible because of the high computational cost. Moreover, the irregular shape of the solid object can make it difficult to generate a mesh of high quality. Instead of re–meshing, it might be more efficient to use a fixed background Cartesian grid and allow the solid object move arbitrarily. In the discontinuous Galerkin framework, this approach has been used for the Poission equation [57] and the Navier–Stokes equation [83]. A generalization to wave propagation problems is of great interests.

6. Summary in Swedish

Vågutbredning är ett fascinerande område som har en mängd vetenskapliga och industriella tillämpningsområden. Redan i urminnes tider användes lurar och horn för att kommunicera över långa avstånd. Detta var ett tidigt tillämpningsområde för akustisk ljudutbredning. Tack vare utnyttjande av elektromagetiska vågor inom telekommunikation kan vi idag avsevärt mycket enklare och snabbare kommunicera med varandra via både ljud och bild. Men vågor kan även ha negativa effekter. Snabba utsläpp av energi i jodens inre kan resultera i seismiska vågor som ger upphov till jordbävningar. Detta kan få förödande konsekvenser för både den enskilde individen och samhället som helhet. Dessa exempel motiverar varför forskning inom vågutbredning är oerhört viktigt.

Rent matematiskt kan vågutbredning modelleras med hjälp av partiella differentialekvationer, där materialens egenskaper beskrivs av koefficienter i ekvationerna. För att lösa dessa ekvationer behövs även randvillkor. Dessa beskriver effekter där vågor interagerar med ränder, som till exempel reflektion och brytningsfenomen. Exakta lösningar (så kallade analytiska lösningar) kan endast tas fram i ett fåtal specialfall. För mer generella fall får vi förlita oss på noggranna approximationer som tas fram med hjälp av att använda numeriska metoder. Dessa numeriska metoder implementeras sedan på moderna och effektiva datorer. Resultatet av dessa blir numeriska simuleringar som ligger till grund för att båda öka vår förståelse för vågutbredning som fenomen och för att svara på viktiga frågeställningar inom vetenskap och teknologi.

Denna avhandling har bidragit till utvecklingen av två kända metoder: finita differenser och diskontinuerlig Galerkin metoden. Finita differenser är effektiva när det gäller att lösa vågutbredningsproblem på kartesiska nät, men har svårigheter när det kommer till att hantera komplexa geometrier och diskontinuiteter i material. För att lösa dessa problem har vi utvecklat en finit differens metod för den akustiska vågekvationen som kan hantera just inhomogeniteter i material samt komplexa geometrier. I denna metod delas beräkningsområdet delas upp i delområden vid materialdiskontinuiteterna. Delområdena kopplas sedan samman numeriskt med hjälp av interpolation. Geometrin hos interfacen och ränder representeras noggrant genom att använda ett kurvlinjärt nät som skapas för varje enskilt delområde. Metoden är energi-stabil och har hög noggranhetsordning.

När man använder finita differenser så är i regel trunkeringsfelet större vid ränderna än i domänens inre för att bevarar stabilitetsegenskaperna. En naturlig frågeställning är därför hur trunkeringsfelet vid randen påverkar den

samlade noggranheten för metoden. För att bestämma noggranhetsordning har vi därför utför normalmodsanalys för den akustiska vågekvationen för en klass av finita differensmetoder i en och två dimensioner.

Diskontinuerliga Galerkin metoder kan vara energistabila och av godtyckligt hög noggranhet. Vidare kan komplexa geometrier representeras noggrant genom att använda ostrukturerade nät. Vi har använd en energi-baserad diskontinuerlig Galerkin metod för att studera och simulera vågutbredning i en domän bestående av ett solitt material som är i kontakt med en vätska.

7. Acknowledgement

When I read a PhD thesis, I usually start reading from this section as I find it interesting to know a bit history of the author. Now it is time to write my own little history. With just a few days left to submit the thesis, I am filled with emotion recalling my PhD journey.

Gunilla Kreiss has been my PhD advisor in the past five years. I feel so lucky that I made the right decision to be your student. I have learned immensely from your broad and deep knowledge in numerical analysis. You have given me much freedom that I did not know how to use in the beginning, but later found valuable on my way to become an independent researcher. When I lost orientation and confidence in the darkness of science, you were supportive and guided me through the tunnel. I am happy to move on, but I certainly will miss you.

I have a second supervisor, Per Lötstedt. Not long after arriving in Uppsala, I was told that you are the master of ODEs. Surely you have helped me in many occasions on that topic. We have not worked together on a project during my PhD, but I got 60 out of 120 credit points from you in my master degree. Thank you for all your help these years. I wish you enjoy your time after retirement.

I got to know Daniel Appelö in my first year as a PhD student. We immediately started a joint work on Hermite methods for the Schrödinger equation, and I am glad that we have finalized the project and got the work published. In ICOSAHOM 2016, instead of sunbathing on Copacabana we derived energy estimates for acoustic–elastic wave propagation problems in the hotel. Since then we have had countless Skype meetings. I thank you very much for bringing me into the world of discontinuous Galerkin methods, which I will continue to explore in the coming years. You are not officially my PhD supervisor, but you are definitely on my list.

It does not feel so long, but it was seven years ago when Michael Thuné greeted me as a new master student at Uppsala University. You later became my teacher in Scientific Computing Bridging Course, and I liked your course very much. Interestingly, I have taught the same course five times as a PhD student. Your teaching style has influenced my teaching philosophy greatly. You are the model of what a brilliant teacher must be.

When I started as a PhD student, Kristoffer Virta was in Gunilla's group. Kristoffer and I had overlaps in research, and we even published a paper together. Thank you Kristoffer, for teaching me MAPLE and answering me many questions about the SBP–SAT methods. Besides scientific computing,

you seem to be very interested in complex analysis and number theory. I wish you success in that path.

I later got the opportunity to collaborate with Anna Nissen. You have much expertise when things go to the Laplace space. It has been a great pleasure to work with you. It was also very nice to visit you in beautiful Bergen, even in the rain, as usual.

Simon Sticko sometimes does not want to be the main person, but is nevertheless the MAIN in this paragraph. You seem to know everything, and have taught me from numerical analysis to programming. I thank you for all your help, and your effort on organizing international symposiums on wave propagation. I wish you immerse in your strongly stable last year and converge to your PhD degree with high order accuracy.

Simon knows everything, so does Martin Almquist. Thank you Martin for discussing many times with me on scientific computing problems, and for always being nice to me. Our discussions have not yet ended up to a publication, but I hope this will happen in the near future.

My research does not overlap much with Hanna Holmgren's, but this does not prevent us having so many interesting talks. More importantly, you have always been helpful and supportive, and I like your view of life.

If I should say something I regret, then it must be that I could not visit Anders Petersson at Lawrence Livermore National Laboratory. Anders and I exchanged so many emails to arrange the visit, and the administration staff Cindy, Linda and Anna–Lena could not be more helpful. It is a huge pity that the visit was cancelled because of non–scientific reasons. I thank you for all your efforts, and I hope to get a chance to visit you in the near future.

There are many other people who have made my PhD time much more enjoyable. Pavol Bauer is my nice officemate from Vienna who knows a lot about food and kids. Lina von Sydow has organized many interesting activities. I have had interesting conversations with Ulrika Jaresund and Loreto Skoknic early in the morning. I also enjoy attending conferences and talking with brilliant researchers, and I hope to see you again. Needless to say, traveling is expensive, and is only possible with the help from several scholarship agencies Åfosk, Liljewalchs, Wallenberg, and Sederholm.

My wife had the ability and desire to become a business women, but to adapt our life you turned to be a professional cook both at home and work. We have had a great time in Uppsala, and I am excited to move to the west with you and our not–yet–born Hamburgare.

I was brought up by my grandmother. Words fail to express my gratitude for that. I wish you return to health. I thank my uncle for his constant help since I was a kid. I wish my parents and grandmother happy.

References

[1] *deal.II*. `http://www.dealii.org`. Accessed: 2017-04-15.

[2] *FEniCS*. `http://www.fenicsproject.org`. Accessed: 2017-04-15.

[3] *Overture*. `http://www.overtureframework.org`. Accessed: 2017-04-15.

[4] *SW4*. `https://geodynamics.org/cig/software/sw4`. Accessed: 2017-04-15.

[5] S. ABARBANEL, A. DITKOWSKI, AND B. GUSTAFSSON, *On error bounds of finite difference approximations to partial differential equations–temporal behavior and rate of convergence*, J. Sci. Comput., 15 (2000), pp. 79–116.

[6] S. ABARBANEL, A. DITKOWSKI, AND A. YEFET, *Bounded error schemes for the wave equation on complex domains*, J. Sci. Comput., 26 (2006), pp. 67–81.

[7] N. ALBIN AND J. KLARMANN, *An algorithmic exploration of the existence of high–order summation by parts operators with diagonal norm*, J. Sci. Comput., 69 (2016), pp. 633–650.

[8] M. ALMQUIST, I. KARASALO, AND K. MATTSSON, *Atmospheric sound propagation over large–scale irregular terrain*, J. Sci. Comput., 61 (2014), pp. 369–397.

[9] D. APPELÖ, J. W. BANKS, W. D. HENSHAW, AND D. W. SCHWENDEMAN, *Numerical methods for solid mechanics on overlapping grids: Linear elasticity*, J. Sci. Comput., 231 (2012), pp. 6012–6050.

[10] D. APPELÖ AND T. HAGSTROM, *An energy–based discontinuous Galerkin discretization of the elastic wave equation in second order form*, Submitted.

[11] D. APPELÖ AND T. HAGSTROM, *A new discontinuous Galerkin formulation for wave equations in second–order form*, SIAM J. Numer. Anal., 53 (2015), pp. 2705–2726.

[12] D. APPELÖ AND G. KREISS, *Application of a perfectly matched layer to the nonlinear wave equation*, Wave Motion, 44 (2007), pp. 531–548.

[13] D. APPELÖ, G. KREISS, AND S. WANG, *An explicit Hermite–Taylor method for the Schrödinger equation*, Commun. Comput. Phys., 21 (2017), pp. 1207–1230.

[14] D. APPELÖ AND N. A. PETERSSON, *A stable finite difference method for the elastic wave equation on complex geometries with free surfaces*, Commun. Comput. Phys., 5 (2009), pp. 84–107.

[15] D. APPELÖ AND N. A. PETERSSON, *A fourth–order accurate embedded boundary method for the wave equation*, SIAM. J. Sci. Comput., 34 (2012), pp. A2982–A3008.

[16] D. APPELÖ AND S. WANG, *An energy based discontinuous Galerkin method for acoustic–elastic waves*, Technical Report.

[17] I. BABUŠKA AND B. Q. GUO, *The h, p and h–p version of the finite element method; basis theory and applications*, Adv. Eng. Softw., 15 (1992), pp. 159–174.

[18] J. W. Banks and T. Hagstrom, *On Galerkin difference methods*, J. Comput. Phys., 313 (2016), pp. 310–327.
[19] J. W. Banks and W. D. Henshaw, *Upwind schemes for the wave equation in second–order form*, J. Comput. Phys., 231 (2012), pp. 5854–5889.
[20] L. Beilina, *Energy estimates and numerical verification of the stabilized domain decomposition finite element/finite difference approach for time–dependent Maxwell's system*, Cent. Eur. J. Math., 11 (2013), pp. 702–733.
[21] E. Burmann, S. Claus, P. Hansbo, M. G. Larson, and A. Massing, *CutFEM: Discretizing geometry and partial differential equations*, Int. J. Numer. Meth. Engng., 104 (2015), pp. 472–501.
[22] M. H. Carpenter, D. Gottlieb, and S. Abarbanel, *Time–stable boundary conditions for finite–difference schemes solving hyperbolic systems: methodology and application to high–order compact schemes*, J. Comput. Phys., 111 (1994), pp. 220–236.
[23] M. H. Carpenter, J. Nordström, and D. Gottlieb, *A stable and conservative interface treatment of arbitrary spatial accuracy*, J. Comput. Phys., 148 (1999), pp. 341–365.
[24] N. Chalmers, L. Krivodonova, and R. Qin, *Relaxing the CFL number of the discontinuous Galerkin method*, SIAM J. Sci. Comput., 36 (2014), pp. A2047–A2075.
[25] X. Chen, D. Appelö, and T. Hagstrom, *A hybrid Hermite–discontinuous Galerkin method for hyperbolic systems with application to Maxwell's equations*, J. Comput. Phys., 257 (2014), pp. 501–520.
[26] C. Chou, C. Shu, and Y. Xing, *Optimal energy conserving local discontinuous Galerkin methods for second–order wave equation in heterogeneous media*, J. Comput. Phys., 272 (2014), pp. 88–107.
[27] E. T. Chung, C. Y. Lam, and J. Qian, *A staggered discontinuous Galerkin method for the simulation of seismic waves with surface topography*, Geophysics, 80 (2015), pp. T119–T135.
[28] M. Ciment and S. H. Leventhal, *Higher order compact implicit schemes for the wave equation*, Math. Comput., 29 (1975), pp. 985–994.
[29] L. Collatz, *The Numerical Treatment of Differential Equations*, Springer, 1966.
[30] D. C. Del Rey Fernández, P. D. Boom, and D. W. Zingg, *A generalized framework for nodal first derivative summation–by–parts operators*, J. Comput. Phys., 266 (2014), pp. 214–239.
[31] D. C. Del Rey Fernández, P. D. Boom, and D. W. Zingg, *Corner–corrected diagonal–norm summation–by–parts operators for the first derivative with increased order of accuracy*, J. Comput. Phys., 330 (2017), pp. 902–923.
[32] D. C. Del Rey Fernández, J. E. Hicken, and D. W. Zingg, *Review of summation–by–parts operators with simultaneous approximation terms for the numerical solution of partial differential equations*, Comput. Fluids, 95 (2014), pp. 171–196.
[33] K. Duru, G. Kreiss, and K. Mattsson, *Stable and high–order accurate boundary treatments for the elastic wave equation on second–order form*,

SIAM J. Sci. Comput., 36 (2014), pp. A2787–A2818.
[34] K. Duru and K. Virta, *Stable and high order accurate difference methods for the elastic wave equation in discontinuous media*, J. Comput. Phys., 279 (2014), pp. 37–62.
[35] T. C. Fisher and M. H. Carpenter, *High–order entropy stable finite difference schemes for nonlinear conservation laws: Finite domains*, J. Comput. Phys., 252 (2013), pp. 518–557.
[36] T. C. Fisher, M. H. Carpenter, J. Nordström, N. K. Yamaleev, and C. Swanson, *Discretely conservative finite–difference formulations for nonlinear conservation laws in split form: Theory and boundary conditions*, J. Comput. Phys., 234 (2013), pp. 353–375.
[37] B. Fornberg, *Calculation of weights in finite difference formulas*, SIAM. Rev., 40 (1998), pp. 685–691.
[38] B. Fornberg and N. Flyer, *A Primer on Radial Basis Functions with Applications to the Geosciences*, SIAM, 2015.
[39] T. P. Fries and T. Belytschko, *The extended/generalized finite element method: An overview of the method and its applications*, Int. J. Numer. Meth. Engng., 84 (2010), pp. 253–304.
[40] G. J. Gassner, *A skew–symmetric discontinuous Galerkin spectral element discretization and its relation to SBP–SAT finite difference methods*, SIAM J. Sci. Comput., 35 (2013), pp. 1233–1253.
[41] G. J. Gassner, A. R. Winters, and D. A. Kopriva, *Split form nodal discontinuous Galerkin schemes with summation–by–parts property for the compressible Euler equations*, J. Comput. Phys., 327 (2016), pp. 39–66.
[42] J. C. Gilbert and P. Joly, *Higher order time stepping for second order hyperbolic problems and optimal CFL conditions*, Springer, 2008, pp. 67–93.
[43] J. Goodrich, T. Hagstrom, and J. Lorenz, *Hermite methods for hyperbolic initial–boundary value problems*, Math. Comput., 75 (2005), pp. 595–630.
[44] W. J. Gordon and C. A. Hall, *Construction of curvilinear co–ordinate systems and applications to mesh generation*, Int. J. Numer. Meth. Eng., 7 (1973), pp. 461–477.
[45] K. F. Graff, *Wave Motion in Elastic Solids*, Dover Publications, 1991.
[46] M. J. Grote, A. Schneebeli, and D. Schötzau, *Discontinuous Galerkin finite element method for the wave equation*, SIAM. J. Numer. Anal., 44 (2006), pp. 2408–2431.
[47] B. Gustafsson, *The convergence rate for difference approximations to mixed initial boundary value problems*, Math. Comput., 29 (1975), pp. 396–406.
[48] B. Gustafsson, *The convergence rate for difference approximations to general mixed initial boundary value problems*, SIAM. J. Numer. Anal., 18 (1981), pp. 179–190.
[49] B. Gustafsson, *High Order Difference Methods for Time Dependent PDE*, Springer, 2008.
[50] B. Gustafsson, H. O. Kreiss, and J. Oliger, *Time–Dependent Problems and Difference Methods*, John Wiley & Sons, 2013.
[51] T. Hagstrom and D. Appelö, *Solving PDEs with Hermite interpolation*,

Lecture Notes in Computational Science and Engineering, 106 (2015), pp. 31–49.
[52] T. Hagstrom and G. Hagstrom, *Grid stabilization of high–order one–sided differencing II: second–order wave equations*, J. Comput. Phys., 231 (2012), pp. 7907–7931.
[53] W. D. Henshaw, *A high–order accurate parallel solver for Maxwell's equations on overlapping grids*, SIAM J. Sci. Comput., 28 (2006), pp. 1730–1765.
[54] J. S. Hesthaven and T. Warburton, *Nodal Discontinuous Galerkin Methods*, Springer, 2008.
[55] J. E. Hicken, D. C. Del Rey Fernández, and D. W. Zingg, *Multidimensional summation–by–parts operators: general theory and application to simplex elements*, SIAM J. Sci. Comput., 38 (2016), pp. A1935–A1958.
[56] G. M. Hulbert and T. J. R. Hughes, *Space–time finite element methods for second–order hyperbolic equations*, Comput. Methods Appl. Mech. Eng., 84 (1990), pp. 327–348.
[57] A. Johansson and M. G. Larson, *A high order discontinuous Galerkin Nitsche method for elliptic problems with fictitious boundary*, Numer. Math., 123 (2013), pp. 607–628.
[58] M. Käser and M. Dumbser, *An arbitrary high–order discontinuous Galerkin method for elastic waves on unstructured meshes–I. the two–dimensional isotropic case with external source terms*, Geophys. J. Int., 116 (2006), pp. 855–877.
[59] M. Käser and M. Dumbser, *A highly accurate discontinuous Galerkin method for complex interfaces between solids and moving fluids*, Geophysics, 73 (2008), pp. T23–T35.
[60] P. Knupp and S. Steinberg, *Fundamentals of Grid Generation*, CRC Press, 1993.
[61] D. A. Kopriva, *Implementing Spectral Methods for Partial Differential Equations*, Springer, 2009.
[62] J. E. Kozdon and L. C. Wilcox, *Stable coupling of nonconforming, high–order finite difference methods*, SIAM J. Sci. Comput., 38 (2016), pp. A923–A952.
[63] H. O. Kreiss and J. Oliger, *Comparison of accurate methods for the integration of hyperbolic equations*, Tellus, 24 (1972), pp. 199–215.
[64] H. O. Kreiss, O. E. Ortiz, and N. A. Petersson, *Initial–boundary value problems for second order systems of partial differential equations*, ESAIM–Math. Model. Num., 46 (2012), pp. 559–593.
[65] H. O. Kreiss and N. A. Petersson, *An embedded boundary method for the wave equation with discontinuous coefficients*, SIAM J. Sci. Comput., 28 (2006), pp. 2054–2074.
[66] H. O. Kreiss and N. A. Petersson, *A second order accurate embedded boundary method for the wave equation with Dirichlet data*, SIAM J. Sci. Comput., 27 (2006), pp. 1141–1167.
[67] H. O. Kreiss, N. A. Petersson, and J. Ystrom, *Difference approximations for the second order wave equation*, SIAM. J. Numer. Anal.,

40 (2002), pp. 1940–1967.
[68] H. O. Kreiss, N. A. Petersson, and J. Yströn, *Difference approximations of the Neumann problem for the second order wave equation*, SIAM. J. Numer. Anal., 42 (2004), pp. 1292–1323.
[69] H. O. Kreiss and G. Scherer, *Finite element and finite difference methods for hyperbolic partial differential equations*, Mathematical Aspects of Finite Elements in Partial Differential Equations, Symposium Proceedings, (1974), pp. 195–212.
[70] H. O. Kreiss and G. Scherer, *On the existence of energy estimates for difference approximations for hyperbolic systems*, Technical Report, Department of Scientific Computing, Uppsala University, (1977).
[71] H. O. Kreiss and L. Wu, *On the stability definition of difference approximations for the initial boundary value problem*, Appl. Numer. Math., 12 (1993), pp. 213–227.
[72] R. J. LeVeque, *Finite Volume Methods for Hyperbolic Problems*, Cambridge University Press, 2002.
[73] T. Lundquist and J. Nordström, *The SBP–SAT technique for initial value problems*, J. Comput. Phys., 270 (2014), pp. 84–104.
[74] K. T. Mandli, A. J. Ahmadia, M. Berger, D. Calhoun, D. L. George, Y. Hadjimichael, D. I. Ketcheson, G. I. Lemoine, and R. J. LeVeque, *Clawpack: building an open source ecosystem for solving hyperbolic pdes*, PeerJ Computer Science, 2 (2016), p. e68.
[75] K. Mattsson, *Summation by parts operators for finite difference approximations of second–derivatives with variable coefficient*, J. Sci. Comput., 51 (2012), pp. 650–682.
[76] K. Mattsson, *Diagonal–norm upwind SBP operators*, J. Comput. Phys., 335 (2017), pp. 283–310.
[77] K. Mattsson and M. Almquist, *A solution to the stability issues with block norm summation by parts operators*, J. Comput. Phys., 253 (2013), pp. 418–442.
[78] K. Mattsson, M. Almquist, and M. H. Carpenter, *Optimal diagonal–norm SBP operators*, J. Comput. Phys., 264 (2014), pp. 91–111.
[79] K. Mattsson and M. H. Carpenter, *Stable and accurate interpolation operators for high–order multiblock finite difference methods*, SIAM J. Sci. Comput., 32 (2010), pp. 2298–2320.
[80] K. Mattsson, F. Ham, and G. Iaccarino, *Stable and accurate wave–propagation in discontinuous media*, J. Comput. Phys., 227 (2008), pp. 8753–8767.
[81] K. Mattsson, F. Ham, and G. Iaccarino, *Stable boundary treatment for the wave equation on second–order form*, J. Sci. Comput., 41 (2009), pp. 366–383.
[82] K. Mattsson and J. Nordström, *Summation by parts operators for finite difference approximations of second derivatives*, J. Comput. Phys., 199 (2004), pp. 503–540.
[83] B. Müller, S. Krämer-Eis, F. Kummer, and M. Oberlack, *A high–order discontinuous Galerkin method for compressible flows with immersed boundaries*, Int. J. Numer. Meth. Engng., 110 (2016), pp. 3–30.

[84] S. NILSSON, N. A. PETERSSON, B. SJÖGREEN, AND H. O. KREISS, *Stable difference approximations for the elastic wave equation in second order formulation*, SIAM J. Numer. Anal., 45 (2007), pp. 1902–1936.
[85] J. NORDSTRÖM, K. FORSBERG, C. ADAMSSON, AND P. ELIASSON, *Finite volume methods, unstructured meshes and strict stability for hyperbolic problems*, Appl. Numer. Math., 45 (2003), pp. 453–473.
[86] J. NORDSTRÖM AND T. LUNDQUIST, *Summation–by–parts in time*, J. Comput. Phys., 251 (2013), pp. 487–499.
[87] J. NORDSTRÖM AND T. LUNDQUIST, *Summation–by–parts in time: the second derivative*, SIAM J. Sci. Comput., 38 (2016), pp. A1561–A1586.
[88] P. OLSSON, *Summation by parts, projections, and stability. I*, Math. Comput., 64 (1995), pp. 1035–1065.
[89] P. OLSSON, *Summation by parts, projections, and stability. II*, Math. Comput., 64 (1995), pp. 1473–1493.
[90] N. A. PETERSSON, O. O'REILLY, B. SJÖGREEN, AND S. BYDLON, *Discretizing singular point sources in hyperbolic wave propagation problems*, J. Comput. Phys., 321 (2016), pp. 532–555.
[91] N. A. PETERSSON AND B. SJÖGREEN, *An energy absorbing far–field boundary condition for the elastic wave equation*, Commun. Comput. Phys., 6 (2009), pp. 483–508.
[92] N. A. PETERSSON AND B. SJÖGREEN, *Stable grid refinement and singular source discretization for seismic wave simulations*, Commun. Comput. Phys., 8 (2010), pp. 1074–1110.
[93] N. A. PETERSSON AND B. SJÖGREEN, *Super–grid modeling of the elastic wave equation in semi–bounded domains*, Commun. Comput. Phys., 16 (2014), pp. 913–955.
[94] N. A. PETERSSON AND B. SJÖGREEN, *Wave propagation in anisotropic elastic materials and curvilinear coordinates using a summation–by–parts finite difference method*, J. Comput. Phys., 299 (2015), pp. 820–841.
[95] A. D. PIERCE, *Acoustics: An Introduction to Its Physical Principles and Applications*, McGraw–Hill, 1981.
[96] G. R. RICHTER, *An explicit finite element method for the wave equation*, Appl. Numer. Math., 16 (1994), pp. 65–80.
[97] R. D. RICHTMYER AND K. W. MORTON, *Difference Methods for Initial–Value Problems*, John Wiley & Sons, 1967.
[98] B. SJÖGREEN AND N. A. PETERSSON, *A fourth order accurate finite difference scheme for the elastic wave equation in second order formulation*, J. Sci. Comput., 52 (2012), pp. 17–48.
[99] S. STICKO AND G. KREISS, *A stabilized nitsche cut element method for the wave equation*, Comput. Methods Appl. Mech. Eng., 309 (2016), pp. 364–387.
[100] B. STRAND, *Summation by parts for finite difference approximations for d/dx*, J. Comput. Phys., 110 (1994), pp. 47–67.
[101] G. STRANG AND G. FIX, *An Analysis of the Finite Element Method*, Wellesley–Cambridge, 2008.
[102] M. SVÄRD AND J. NORDSTRÖM, *Review of summation–by–parts schemes for initial–boundary–value problems*, J. Comput. Phys., 268 (2014), pp. 17–38.
[103] V. THOMÉE, *From finite differences to finite elements A short history of*

numerical analysis of partial differential equations, J. Comput. Appl. Math., 128 (2001), pp. 1–54.
[104] L. L. THOMPSON AND P. M. PINSKY, *A space–time finite element method for structural acoustics in infinite domains Part 1: Formulation, stability and convergence*, Comput. Methods Appl. Mech. Eng., 132 (1996), pp. 195–227.
[105] K. VIRTA AND K. MATTSSON, *Acoustic wave propagation in complicated geometries and heterogeneous media*, J. Sci. Comput., 61 (2014), pp. 90–118.
[106] S. WANG, *An improved high order finite difference method for non–conforming grid interfaces for the wave equation*, in review, available as preprint arXiv:1702.02056.
[107] S. WANG AND G. KREISS, *Convergence of summation–by–parts finite difference methods for the wave equation*, J. Sci. Comput., 71 (2017), pp. 219–245.
[108] S. WANG, A. NISSEN, AND G. KREISS, *Convergence of finite difference methods for the wave equation in two space dimensions*, in review, available as preprint arXiv:1702.01383.
[109] S. WANG, K. VIRTA, AND G. KREISS, *High order finite difference methods for the wave equation with non–conforming grid interfaces*, J. Sci. Comput., 68 (2016), pp. 1002–1028.
[110] T. WARBURTON AND T. HAGSTROM, *Taming the CFL number for discontinous Galerkin methods on structured meshes*, SIAM J. Numer. Anal., 46 (2008), pp. 3151–3180.
[111] G. B. WHITHAM, *Linear and Nonlinear Waves*, John Wiley & Sons, 1974.
[112] L. C. WILCOX, G. STADLER, C. BURSTEDDE, AND O. GHATTAS, *A high-order discontinuous Galerkin method for wave propagation through coupled elastic-acoustic media*, J. Comput. Phys., 229 (2010).

Acta Universitatis Upsaliensis

Digital Comprehensive Summaries of Uppsala Dissertations from the Faculty of Science and Technology 1522

Editor: The Dean of the Faculty of Science and Technology

A doctoral dissertation from the Faculty of Science and Technology, Uppsala University, is usually a summary of a number of papers. A few copies of the complete dissertation are kept at major Swedish research libraries, while the summary alone is distributed internationally through the series Digital Comprehensive Summaries of Uppsala Dissertations from the Faculty of Science and Technology. (Prior to January, 2005, the series was published under the title "Comprehensive Summaries of Uppsala Dissertations from the Faculty of Science and Technology".)

Distribution: publications.uu.se
urn:nbn:se:uu:diva-320614

ACTA
UNIVERSITATIS
UPSALIENSIS
UPPSALA
2017